FAST-NEUTRON RADIOLYSIS OF HEAVY WATER

by

SAMPATH SADHU KUMAR

B. Sc. (Tech.), MADRAS UNIVERSITY, INDIA, 1956.

A MASTER'S THESIS

submitted in partial fulfillment of the

requirements for the degree

MASTER OF SCIENCE

Department of Nuclear Engineering

KANSAS STATE UNIVERSITY
Manhattan, Kansas

1967

Approved by:

Richard E. Faw

Major Professor

CONTENTS

INTRODUCTION..... 1

OBJECTIVE..... 21

THEORY..... 23

DESCRIPTION OF APPARATUS..... 36

EXPERIMENTAL PROCEDURE..... 48

PRESENTATION OF DATA AND DATA ANALYSIS..... 53

RESULTS AND CONCLUSIONS..... 59

ACKNOWLEDGEMENT..... 67

REFERENCES..... 68

APPENDIX A: Average Energy of the Deuteron Source Spectrum..... 72

APPENDIX B: Determination of a Best Value of the Extinction Coefficient. 74

APPENDIX C: Raw Data and Calculations of Gamma Radiolysis..... 76

APPENDIX D: Raw Data of the Fast-Neutron Radiolysis Experiment..... 79

APPENDIX E: Statistical Analysis of the Raw Data of the Fast-Neutron Radiolysis Experiment..... 82

APPENDIX F: Relative Nuclear Target Density for Scattering of Neutrons Created in the (n,2n) Reaction..... 87

LIST OF TABLES

1. Energy Distribution in Fast-Neutron Radiolysis of Water..... 16

2. Calculated Energy Distribution in Deuteron-Neutron Interactions..... 27

3. Calculated Energy Distribution in Fast-Neutron Radiolysis of Heavy Water..... 28

4. Fractional Energy Deposition by Secondary Charged Particles..... 29

5. An Estimate of $G(Fe^{3+})$-Value for Fast-Neutron Radiolysis of Heavy Water..... 31

6. An Estimate of $G(Fe^{3+})$-Value for Fast-Neutron Radiolysis of Light Water..... 31

7. Absorbances of Standard Ferric Solutions..... 53

8. Absorbances in Fast-Neutron Radiolysis..... 57

9. Comparison of the Values of the Extinction Coefficient for Fe^{3+} in 0.8N H_2SO_4 at 25°C..... 59

10. Comparison of the Ratio of G-Values for Gamma Radiolysis..... 60

LIST OF FIGURES

1. Differential cross-section for n-d elastic scattering..... 25
2. Plot of $\sigma(\tau)$ vs. τ for n-d elastic scattering..... 26
3. Plot of $G(Fe^{3+})$ vs. ILET for Fricke dosimetric solution..... 30
4. Schematic diagram of the neutron generator..... 38
5. A view of the neutron generator..... 39
6. A view of the control console of the neutron generator..... 41
7. Sample holder for fast-neutron radiolysis..... 42
8. A view of the "Gammacell"-220..... 45
9. Schematic diagram of the spectrophotometer..... 46
10. Plot of absorbance vs. ferric ion concentration..... 55

NOMENCLATURE†

A	Absorbance
A_h	Absorbance of heavy water solution
A_i	Absorbance in the i^{th} run or of the i^{th} solution
A_{ij}	Absorbance of the j^{th} sample in the i^{th} run
A_{ijk}	Absorbance in the k^{th} trial of the j^{th} sample in the i^{th} run
A_ℓ	Absorbance of light water solution
C	Concentration, moles per liter
C_i	Concentration of the i^{th} solution, moles per liter
D	Absorbed dose, rads
D_1	Absorbed dose in material 1, rads
D_2	Absorbed dose in material 2, rads
D_a	Absorbed dose in air, rads
D_d	Absorbed dose in the dosimetric solution, rads
D_m	Absorbed dose in a material, rads
E_n	Energy of incident neutron, Mev.
e	Energy absorbed per gram of the irradiated sample, ev. per gram
f_i	Fraction of energy deposited by a secondary charged particle created in the i^{th} interaction
G	G-value of a product, molecules per hundred ev.
G_i	G-value of a product due to the energy loss of a secondary charged particle created in the i^{th} interaction, molecules per hundred ev.

† This nomenclature is not applicable to Appendix E.

L	Length of optical path, centimeters
M	Mass of target nucleus, amu
N	Target nuclear density, number of atoms per cubic centimeter
N_d	Deuterium atom density, number of atoms per cubic centimeter
N_i	Target nuclear density for the i^{th} interaction, number of atoms per cubic centimeter
N'_i	Relative target nuclear density
n	Number of molecules of the product formed per gram of the sample irradiated, molecules per gram
R	Sum of the squares of the errors r
R_o	Radius of container, centimeters
r	Set of experimental errors in absorbance readings
S_v	Volumetric source strength, number of neutrons per cubic centimeter per second
"t"	Student's t
ε	Extinction coefficient, liters per mole centimeter
θ	Angle of scattering in the center-of-mass system, degrees
μ	Mass energy absorption coefficient, square centimeters per gram
μ_a	Mass energy absorption coefficient of air, square centimeters per gram
μ_d	Mass energy absorption coefficient of dosimetric solution, square centimeters per gram
μ_m	Mass energy absorption coefficient in a material, square centimeters per gram
ρ	Density, grams per cubic centimeter
ρ_1	Density of material 1, grams per cubic centimeter

ρ_2	Density of material 2, grams per cubic centimeter
σ	Cross-section for neutron interaction, barns
σ_i	Cross-section for the i^{th} interaction, barns
$\sigma(\tau)$	Differential cross-section per unit energy for an energy loss τ, barns per Mev.
$\sigma(\Omega)$	Differential cross-section per unit solid angle for scattering in the direction Ω, barns per steradian
$\bar{\sigma}_i^2$	Variance of the i^{th} quantity
τ	Energy of secondary charged particle, Mev.
$\bar{\tau}$	Average energy of the source spectrum of a secondary charged particle, Mev.
$\bar{\tau}_i$	Average energy of the source spectrum of a secondary charged particle created in the i^{th} interaction, Mev.
ϕ_{max}	Maximum secondary neutron flux, number per square centimeter per second
Ω	Solid angle, steradians

INTRODUCTION

This research is in the area of radiation chemistry, which may be defined as the chemistry of reactions initiated in a system by the passage of ionizing radiation. The immediate effect of passage of ionizing radiation through matter is the generation of electronically excited species and ions. These products are usually unstable and undergo a series of transformations. The dissociation of excited molecules and certain reactions of ions lead to the formation of free radicals. Free radicals may be defined as atoms or molecules having one or more unpaired electrons available for the formation of chemical bonds. The formation of free radicals is followed by diffusion and chemical reaction. Thus, the over-all effect of absorption of radiation energy is the appearance of a new chemical by transformation of a chemical initially present.

Radiation chemistry can be said to have originated with the discovery of X rays by Roentgen and of radioactivity by Becquerel shortly thereafter (3). One of the earliest reactions to have been observed was the action of radiation from radium on water. The first quantitative work seems to have been done by Lind (29), who studied the formation of ozone in oxygen under the influence of alpha radiation. Until about 1942, radiation chemistry did not attract many scientists. Afterwards, with the development of atomic energy programs, a variety of particle accelerators and cheap artificially-made isotopes were made available to the radiation chemist. At present, this branch of science is studied extensively both because of its intrinsic interest and because of its practical value in the fields nuclear energy, radiobiology and radiation processing.

As already mentioned, the passage of ionizing radiation through matter triggers a number of processes. The entire process can be said to follow a sequence of three stages: (a) the physical stage, (b) the physicochemical stage, and (c) the chemical stage (32).

The physical stage consists of the deposition of energy in the system. Its duration is of the order of 10^{-15} seconds. In the physicochemical stage, processes leading to the establishment of thermal equilibrium take place, the duration being of the order of 10^{-12} seconds. The chemical stage consists of diffusion and chemical reaction among the reactive species and terminates with the establishment of chemical equilibrium. Its duration ranges from 10^{-8} seconds upwards, depending on diffusion rates and reaction rates of the reactants.

The analysis of the physical stage requires a knowledge of the interactions of radiation with matter and the mechanism of slowing-down of charged particles. A detailed discussion of the interaction of radiation with matter is beyond the scope of this work. It is known that charged particles cause ionization directly in the medium through which they pass. Gamma rays and X rays create energetic electrons by certain mechanisms; ionization is caused by these electrons. Neutrons interact exclusively with atomic nuclei and create energetic charged particles, neutrons and electromagnetic radiation.

Charged particles, irrespective of their origin, give rise to a trail of excited and ionized species while slowing down in matter. Excited states are produced when bound electrons in atoms and molecules gain energy and are raised to higher energy levels. Ions are produced when the energy gained is sufficient and the transient excited states produced are such that the electrons are expelled. It is not only the total energy deposited that is

of interest, but also the spatial distribution of energy loss. The importance of spatial distribution of energy loss can be recognized from the fact that the result of energy deposition is the formation of clusters of excited and ionized species.

The rate of change of energy of a charged particle with the distance traversed by it is termed linear energy transfer and is written as LET. It is also called the stopping power of the charged particle in the medium of concern. LET has been found to be a useful parameter in the analysis of chemical effects of radiation.

The cluster of excited and ionized species formed in the track of a charged particle is called a spur. The basic view of radiation chemists is that the track of an energetic charged particle is formed of a string of spherically symmetric spurs of ions and excited species, which eventually lead to the formation of free radicals. The distribution of these spherical spurs along the track is primarily determined by the LET of the charged particle.

On the tracks of low LET charged particles, the spurs are sufficiently separated and do not interact with each other. The mode of ionization caused by low LET charged particles is called spur ionization. For high values of LET the spherical spurs are sufficiently close together that, over a distance of many spurs, the track becomes a cylinder of active species with practically no variation in concentration (26). The mode of ionization caused by high LET particles is termed columnar ionization.

In the track zones of charged particles, the concentration of free radicals is high; the greater the LET, the greater is the radical concentration.

Hence, radical-radical reactions take place with high probability in these zones. As the tracks or spurs expand by diffusion, the radicals have a chance to meet other species. The yield from radical-radical reactions is usually called the molecular yield, while the yield of radicals escaping into the bulk of the medium is called the free radical yield. From this elementary picture, it may be seen that a high LET radiation gives rise to higher molecular yields, whereas a low LET radiation favors higher free radical yields. The relative proportions of molecular and free radical yields influence the final quantitative chemical yield. Thus, the LET of a particle affects the chemical yield resulting from the deposition of energy by the particle. However, the situation is not as simple as depicted here. This is merely a broad generalization to bring out the importance of LET.

Among the several factors which complicate the analysis of radiation-induced chemical effect, mention will be made about one in particular. The electrons ejected as a consequence of ionization caused by radiation may themselves be sufficiently energetic to produce further ionization and excitation. Some of these electrons will have enough energy to travel far from the original site of ionization; they form tracks of their own, branching off from the primary track. Such electrons are known as delta rays. It is known that high LET particles lose part of their energy by creating delta rays which are generally low LET particles. Thus, although the high LET particles primarily give rise to lower free radical yields, the low LET particles which are the offshoot of the high LET particles tend to boost the free radical yield. However, in general it can be said that the chemi-

cal change attributable to the free radical yield will be greater in the case of low LET radiation than that in the case of high LET radiation.

The foregoing discussion shows that a knowledge of LET is a necessity for the radiation chemist. The computation of LET is complicated by two facts: (a) the LET is a continuously varying quantity and (b) the energy lost by the primary particle in a particular section of the track is not necessarily absorbed locally, but may be transferred in part to delta rays or to secondary electromagnetic radiation. Several authors have dealt with the topic of linear energy transfer, prominent among them being Bethe and Ashkin (10) and Rossi (35). The theory section of this thesis shows the utility of LET in a specific manner.

The analysis of the physicochemical stage requires a knowledge of the reactions of excited atoms, molecules and ions. Discussion of these reactions is beyond the scope of this work. Reference (3) gives a good description of these reactions. During this stage, the excited species dissipate their energy by such processes as bond rupture, luminescence, internal conversion and energy transfer.

Another phenomenon of interest during the physicochemical stage is the fate of the low energy electrons produced simultaneously with the positive ions during the physical stage. These electrons are born with kinetic energies as low as a few electron volts. These energies propel them to a short distance away from the parent ion. At this stage, several possibilities arise.

Platzman (33) has shown that electrons lose energy in a medium much more slowly, once they have fallen to an energy below that of the lowest excita-

tion energy of the atoms of the medium (about 0.5 to 4 ev.). These electrons have comparatively long lifetimes and are termed subexcitation electrons (3). Subexcitation electrons are likely to be important in systems containing one or more minor components which have a lower excitation energy than the principal component. In such systems, radiolytic reactions of the excited minor component assume significance. Platzman has estimated that for high energy radiations about 15 to 20 percent of the absorbed energy might be dissipated by the subexcitation electrons.

The physicochemical stage is followed by the chemical stage. During this stage, the chemically reactive species undergo chemical transformations as they start diffusing away from the track zones or spurs. Two important problems associated with this stage have been examined theoretically: one of them has to do with the question of the relative importance of ionic against free radical reactions; the other is associated with the spatial inhomogeneity of the initial distribution of reactive species.

It was thought in the earlier days of radiation chemistry that ions were the only active chemical species produced by ionizing radiation. Subsequent work contradicted this view to such an extent that it was given up. However, very recent experiments have proved that ions do have a significant role in radiation-reaction mechanisms. The present belief is that ionic reactions cannot be overlooked in gas-phase systems; but in condensed systems, the main reactive species produced in the physiochemical stage and which react in the chemical stage are free radicals (27).

The mathematical analysis of radiation-induced chemical processes is not the same as that used for conventional chemical processes. In a conventional

process, the concentrations of reactants are generally uniform throughout the entire volume of the system and are dependent only on the time variable. In radiation-induced processes in liquids, the concentrations depend not only on time, but also on position in the system. The spatial and temporal dependences are governed by factors such as the type of ionization (spur or columnar), initial distribution of radicals, diffusion coefficients and rate constants. The analysis of these processes is known as diffusion kinetics. Several scientists, notably Kuppermann and Belford (26) have successfully employed this analysis.

With the establishment of chemical equilibrium, the radiation-initiated processes come to an end. The task of the radiation chemist is to estimate quantitatively the chemical change induced by radiation. To aid quantitative comparison of effects, reaction yields are expressed in terms of the numbers of molecules converted per 100 ev. of energy absorbed. Yields thus defined are called G-values (3). Thus, G(X) refers to the number of molecules of a product, X, formed on irradiation per 100 ev. of energy absorbed, and G(-Y) refers, in the same way, to the loss of material, Y, that is destroyed on irradiation. The symbol G_Z is used to denote the earliest detectable yield of Z, as it emerges from the spurs. The use of G-values has the advantage that it does not imply that the chemical action is controlled by the number of ions formed. G-values have now become the customary means of expressing radiation-chemical yields.

The definition of G-value implies estimation of the energy absorbed. The techniques of dose determination constitute the field of radiation dosimetry. Many techniques have been developed and reference (3) gives a good

survey of them. In chemical dosimetry, the radiation dose absorbed in a system is determined from the observed chemical change produced in the system. Of the chemical dosimeters developed, the Fricke, or ferrous sulfate, dosimeter is probably the most widely used. The reaction involved in the Fricke dosimeter is oxidation of an acid solution of ferrous sulfate to the ferric salt, in the presence of dissolved oxygen and under the influence of radiation.

At present, the actions of ionizing radiation on a variety of chemical systems is well known. The radiation chemistry of water and aqueous solutions has been the subject of a great deal of experimental and theoretical study. The interest in water arises partly from its relative simplicity and partly because aqueous systems are of special interest in radiobiology and reactor technology. The development of ideas on reaction mechanisms in water is described by Hart (18).

In liquid water, as in any other medium, ionizing radiation produces excited and ionized species. The excited molecules may dissociate to form radical pairs or ion pairs or may revert to the ground state through radiationless transitions. It is generally believed that ion pair formation is the predominant effect. Most of the radical pairs formed by dissociation of excited molecules recombine without producing appreciable over-all chemical change.

Mass spectrometric analysis of irradiated water vapor shows the presence of a variety of positive ions. It is reasonable to infer the presence of these ions in irradiated liquid water too. However, because of the caging effect of liquid molecules, these ions undergo such transformations (3) that

all ions, other than H_2O^+, can be ignored in the final analysis. Hence, the ionizing action in liquid water can be represented by the equation:

$$H_2O \rightarrow H_2O^+ + e^-.$$

The fate of the electron has been subject to much investigation. If the electron is sufficiently energetic it forms a delta track; if not, it travels only a short distance away from the parent ion.

There are two theories concerning the fate of this low energy electron in water. According to Samuel and Magee (38), a 10 ev. electron will travel a distance of about 20 Å before it reaches thermal energy. At this distance, the electron will still be within the electrostatic field of the positive ion. Hence, it will be drawn back to the ion and the ion will be neutralized. The product of neutralization is a highly excited water molecule which will dissociate into a hydrogen and a hydroxyl radical:

$$H_2O^+ + e^- \rightarrow H_2O^{**} \rightarrow H^\cdot + OH^\cdot.$$

Thus, according to Samuel and Magee, passage of radiation through liquid water results in spurs or columns of the radicals close to the track; there is no difference in the initial distribution of hydrogen and hydroxyl radicals.

Platzman (34) considered the energy loss of a secondary electron and concluded that a 10 ev. electron in water would travel at least 50 Å from the positive ion before being reduced to thermal energy. At this distance, it would essentially be free of the electrostatic attraction of the parent ion. The electron becomes "solvated" and retains this identity until it enters

into chemical reactions. The term "solvation" is rather difficult to define. The electron attracts several water molecules around it and orients them according to the electrostatic attraction between it and the water dipoles. In chemical reactions, a solvated electron acts like a hydrogen atom. (A solvated ion, or electron is considered to be more reactive in that it can enter into endothermic reactions by virtue of the solvation energy.) The parent ion yields a hydroxyl radical by neutralization:

$$H_2O^+ + OH^- \rightarrow H_2O + OH^{\cdot}.$$

Hence, according to Platzman, the distribution of hydroxyl radicals is different from that of the solvated electrons or hydrogen atoms; the hydrogen atoms are more spread out than the hydroxyl radicals. This view seems to be plausible from the fact that in most cases the G_H-value is higher than the G_{OH}-value in radiolysis of water. The model of Samuel and Magee may fit in other systems in which the migration length of the electron is small.

The relative importance of solvated electrons and hydrogen atoms has been the subject of a great deal of study. At present, the following conclusions have been reached (39, 3).

(a) It is established that the primary reducing species in aqueous irradiated solutions are the solvated electrons or, possibly, a mixture of solvated electrons and hydrogen atoms.

(b) In most cases, solvated electrons produce the same products as hydrogen atoms, the possible difference being in the reaction rates.

(c) The pH of the solution determines the relative importance of these

two species. It has been observed that, in solutions with pH above 3, the solvated electron plays the major role. In solutions with pH less than 3, the hydrogen atom seems to be entirely dominant. This may be due to the transformation of the solvated electron by the rapid reaction:

$$e^-_{aq} + H^+ \rightarrow H^\cdot .$$

The Fricke dosimetric solution has a very low pH and it is reasonable to assume that the primary active species remaining at the end of the physicochemical stage are the hydrogen and hydroxyl radicals.

In the chemical stage, the radicals react among themselves or diffuse and react with the substrate. In the spurs or columnar track zones, the initial radical concentrations are high and radical-radical reactions take place with great probability. The reactions are:

$$H^\cdot + OH^\cdot \rightarrow H_2O,$$

$$H^\cdot + H^\cdot \rightarrow H_2,$$

and

$$OH^\cdot + OH^\cdot \rightarrow H_2O_2.$$

As the spurs or zones expand by diffusion, the radicals spread out. They get more opportunities to react with other species than to react among themselves. Hydrogen and hydrogen peroxide formed by the above reactions are called molecular products. The radicals which diffuse and are free to react with other species constitute the radical yield.

From the above analysis, it is seen that the radiolytic decomposition

of water leads to the formation of H_2, H_2O_2, $H^\cdot$ and $OH^\cdot$. Since, for every $H^\cdot$ atom initially formed an $OH^\cdot$ radical is formed, it should be possible to specify the decomposition in terms of either of these two radicals. The total yield of hydrogen atoms, not including those which recombine with hydroxyl radicals to form water, is the sum of the radical yield, G_H' and twice the molecular yield, G_{H_2}. Hence, the decomposition is characterised by the relationship:

$$G_{-H_2O} = G_H + 2G_{H_2} = G_{OH} + 2\,G_{H_2O_2},$$

where G_{-H_2O} stands for the net number of water molecules decomposed. The final chemical yield depends upon the nature of the solute present, pH, presence of oxygen and a host of other factors. Here, discussion is confined to the chemical effect in the Fricke dosimetric solution.

The oxygen in the Fricke dosimetric solution is a very efficient scavenger for hydrogen atoms, combining with them to give the perhydroxyl radicals. (Substances which have a great affinity for a particular radical and which transform the radical speedily are called scavengers.) The reaction is:

$$H^\cdot + O_2 \rightarrow HO_2^\cdot.$$

The $HO_2^\cdot$ radical is not as reactive as the $H^\cdot$ atom. It is, however, a strong oxidizing agent and oxidizes three ferrous ions as shown below:

$$HO_2^\cdot + Fe^{2+} \rightarrow Fe^{3+} + HO_2^-;$$

$$HO_2^- + H^+ \rightarrow H_2O_2;$$

$$H_2O_2 + Fe^{2+} \rightarrow Fe^{3+} + OH^- + OH^{\cdot};$$

$$OH^{\cdot} + Fe^{2+} \rightarrow Fe^{3+} + OH^-.$$

The OH^- ions are neutralized to form water.

The H_2O_2 formed as a molecular product in the tracks oxidizes two ferrous ions as shown below:

$$H_2O_2 + Fe^{2+} \rightarrow Fe^{3+} + OH^- + OH^{\cdot}$$

$$OH^{\cdot} + Fe^{2+} \rightarrow Fe^{3+} + OH^-.$$

The $OH^{\cdot}$ radical of the radical yield converts one ferrous ion by the reaction:

$$OH^{\cdot} + Fe^{2+} \rightarrow Fe^{3+} + OH^-.$$

Thus, the G-value for ferric ions in water is related to the G-values for the free radicals and molecular products:

$$G(Fe^{3+}) = 3G_H + 2G_{H_2O_2} + G_{OH^{\cdot}}$$

Since

$$G_H + 2G_{H_2} = G_{OH} + 2G_{H_2O_2},$$

$$G(Fe^{3+}) = 2[2G_H + G_{H_2}].$$

The $G(Fe^{3+})$-values in water for several types of radiation are tabulated in reference (3).

The radiolysis of water by cobalt-60 gamma rays (1.25 Mev.) has been

investigated by many workers (19, 21, 28). The $G(Fe^{3+})$-value is generally taken as 15.5 or 15.6. In water, the gamma rays undergo Compton scattering and the energetic electrons, so formed, act as the secondary charged particles.

The fast-neutron radiolysis of water (14.6 Mev.) has been studied experimentally (5, 6). The G-value has been reported as 11.5 ± 1.8 in reference (6) and as 10.5 ± 0.2 in reference (5). In water, neutrons react with the oxygen and hydrogen nuclei and give rise to a variety of charged particles. Following is a brief discussion of these interactions.

The interactions of neutrons with oxygen nuclei are: (a) elastic scattering, (b) inelastic scattering, (c) (n,p) reaction and (d) (n,α) reaction. By elastic scattering, the neutron transfers part of its energy to the oxygen nucleus. This is a heavy charged particle, has a high LET and loses energy rapidly by columnar ionization. The inelastic scattering produces an energetic oxygen nucleus and a spectrum of gamma rays. The gamma rays lose energy by Compton scattering. The (n,p) reaction is represented by the equations:

$$ {}_8O^{16} + {}_0n^1 \rightarrow {}_7N^{16} + {}_1H^1, $$

$$ {}_7N^{16} \xrightarrow{\beta^-} {}_8O^{16}. $$

The charged particle of importance is the proton. The N^{16} nucleus loses its kinetic energy by columnar ionization. The radioactive decay of N^{16} produces a continuous spectrum of electrons which lose energy by spur ionization. The (n,α) reaction is represented by the equation:

$$_{8}O^{16} + _{0}n^{1} \rightarrow _{6}C^{13} + _{2}He^{4}.$$

The alpha particle carries away bulk of the energy. The carbon-13 nucleus loses its energy by columnar ionization.

Neutrons interact with the hydrogen nuclei by elastic scattering. A spectrum of protons is produced. The bulk of the energy lost by the neutron is transferred to this proton.

The calculations of energy distribution are based on first collision density. The thickness of the sample is assumed to be small compared to the mean free path of the 14.6 Mev. neutron, but large compared to the ranges of the secondary charged particles. Table 1, which is taken from reference (6), summarizes the energy distribution for fast-neutron radiolysis of water. Considering only the major energy carriers, their LETs and the relative amounts of energy carried by them, it is possible to make an estimate of the G-value (1).

Isotopic substitution of an element in a compound produces certain effects which may generally be termed as isotopic effects. The differences arise in the zero point energies, bond energies, ionization potentials or in certain nuclear properties. It is of interest to investigate the effect on G-value of isotopic substitution. Comparison of the radiolysis of water and heavy water throws some light on this aspect. The interest in the radiolysis of heavy water is also due to the fact that heavy water is an important component in certain nuclear reactor systems.

The G-value in heavy water for gamma radiolysis has been experimentally determined (45, 30, 17). The mode of interaction is Compton scattering.

Table 1. Energy Distribution in Fast-Neutron Radiolysis of Water[a]

1	2[b]	3[c]	4[d]	5	6[e]	7[f]
Interaction, i	N'_i	σ_i	$\bar{\tau}_i$	$N'_i\sigma_i\bar{\tau}_i$	f_i	Particle
$O^{16}(n,n)O^{16}$	1/3	0.73	0.39	0.095	0.021	O^{16}
$O^{16}(n,n')O^{16}$	1/3	0.51	1.15	0.194	0.043	O^{16}
$O^{16}(n,p)O^{16}$	1/3	0.04	4.7	0.064	0.014	p
$O^{16}(n,\alpha)O^{16}$	1/3	0.31	7.8	0.81	0.181	α
$H^1(n,n)H^1$	2/3	0.68	7.3	3.31	0.740	p

[a] Taken from reference (6).

[b] N'_i is relative target nuclear density.

[c] σ_i is the cross-section for the i^{th} interaction, barns. Taken from reference (24).

[d] $\bar{\tau}_i$ is the average energy lost by the neutron, Mev.

[e] f_i is equal to $\frac{N'_i\sigma_i\bar{\tau}_i}{\sum(N'_i\sigma_i\bar{\tau}_i)}$. This is the fraction of energy deposited via the i^{th} interaction.

[f] This is the significant secondary charged particle.

Compton electronic absorption coefficients are independent of the atomic number of the stopping material. The electronic densities of water and heavy water are almost equal. Hence, the energy loss per unit volume must nearly be the same in both cases. However, it has been found that the G-value in heavy water is about 10 percent greater than that in water. This difference is thought to be due to the difference in the migration lengths of electrons in the two media (3).

It is believed (3) that, due to the longer dielectric relaxation time in heavy water, electrons travel farther from the parent ion in heavy water. This means that the $D^{\cdot}$ atoms are much more spread out in heavy water than are the $H^{\cdot}$ atoms in water. This naturally leads to a higher radical yield and higher G-values in heavy water. According to the Platzman model, $H^{\cdot}$ atoms are more widely distributed than are the $OH^{\cdot}$ radicals. If deuterium atoms are much more spread out, the following relationships are to be expected:

$$\frac{G_D}{G_{OD}} > \frac{G_H}{G_{OH}} > 1$$

and

$$\frac{G_{D_2O_2}}{G_{D_2}} > \frac{G_{H_2O_2}}{G_{H_2}} > 1.$$

The data from 220 kvp X-radiolysis bear these relationships and thus lend support to the above view on isotopic effect.

The fast-neutron radiolysis of heavy water is the subject of this

thesis. The interactions between oxygen nuclei and neutrons are the same as those described in the case of water. Fast neutrons react with deuterium nuclei in two ways: (a) elastic scattering and (b) (n,2n) reaction.

The elastic scattering produces energetic deuterons in a continuous energy spectrum. The neutron scattering is peaked in the forward direction. The energetic deuterons (secondary charged particles) lose their energies by ionization and excitation while slowing down in the medium.

The (n,2n) reaction is represented by the equation:

$$_1H^2 + {}_0n^1 \rightarrow {}_1H^1 + 2{}_0n^1 - 2.23 \text{ Mev.}$$

This reaction has been investigated by many scientists (12, 22, 23, 25). However, information on the experimentally determined differential cross-sections are available only up to a proton emission angle of 55^o in the laboratory system (12). Rough calculations, based on this information, showed that scattering into the solid angle cone corresponding to 55^o accounted for a total cross section of 60 millibarns. On the other hand, the total cross-section for the above reaction is 200 millibarns as given in reference (24). Hence, it was concluded that the average energy of the protons cannot possibly be calculated from the available data on differential cross-sections.

As a next best alternative, an approximate analysis of this reaction was carried out with the following assumptions: (a) protons are created at an average energy of 4.12 Mev.; (b) the product neutrons are of equal energies, 4.12 Mev.; (c) these neutrons contribute to the first collision

density; (d) all interactions of these neutrons, other than the n-d elastic scattering are of negligible importance; and (e) the n-d elastic scattering is isotropic.

From the foregoing discussion, it follows that the secondary charged particles created through the (n,2n) reaction are the protons with an average energy of 4.12 Mev. and the deuterons with an average energy of 1.83 Mev.

The uncertainty in the energy distribution of the (n,2n) reaction introduces a corresponding uncertainty in the estimation of the absorbed dose in heavy water exposed to fast neutrons. In view of this, the results of the fast-neutron radiolysis experiment are expressed (in this thesis) in a form which will enable a precise calculation of the $G(Fe^{3+})$-value when a precise calculation of the energy distribution can be performed.

Allen (1) has plotted the variation of $G(Fe^{3+})$-value in light water as a function of the initial LET of the secondary charged particle depositing its energy in water. As far as the chemical reactions of the free radicals are concerned, no difference exists between the radiolysis of light water and that of heavy water. In this thesis, Allen's plot is utilized to make a rough estimate of the $G(Fe^{3+})$-value for the fast-neutron radiolysis of heavy water. This estimate is limited by two facts: (a) the possible isotopic effect is not taken into consideration and (b) the energy distribution calculations are based on the approximate analysis of the (n,2n) reaction.

In this thesis, the terms G-value and $G(Fe^{3+})$-value are used interchangeably. G-values for water or heavy water refer to the $G(Fe^{3+})$-values in

0.8 N sulfuric acid solution of water or heavy water. The terms water and light water are used interchangeably.

OBJECTIVE

The object of this research is to determine experimentally the $G(Fe^{3+})$-value for heavy water on radiolysis by 14.6 Mev. neutrons. A comparison of the G-value estimated from theoretical considerations with the experimentally determined value is also of interest.

The absorbed radiation dose is determined with the aid of a Fricke chemical dosimeter and a spectrophotometer. In order to obtain the G-value, the following experiments are to be performed:

(a) Extinction coefficient for ferric ions: The absorbance of ferric solutions of known concentrations are measured in the spectrophotometer and the extinction coefficient is obtained by applying Beer's law. Using this extinction coefficient, the concentration of any sample can be determined by measuring its absorbance. The extinction coefficients for ferric ions in water and heavy water are not the same, but differ slightly. In this program, the extinction coefficient in heavy water is not determined experimentally; it is calculated from the known ratio of the extinction coefficients in the two media.

(b) $G(Fe^{3+})$-value for heavy water on gamma radiolysis: In order to insure that the experimental techniques adopted are satisfactory, this G-value is determined and compared with published results. The absorbed dose is determined by measuring the chemical change in the Fricke dosimetric solution, the G-values for which is known.

(c) $G(Fe^{3+})$-value for heavy water on fast-neutron radiolysis: Water and heavy water are irradiated with 14.6 Mev. neutrons under identical conditions, so that both are exposed to the same average flux. From the energy loss calculation based on first collision density and the absorbances of the irradiated solutions measured in the spectrophotometer, the ratio of the G-values in heavy water and light water can be calculated. The result of this experiment is presented as the ratio of absorbances of heavy water and light water so that it does not carry with it the uncertainties associated with the calculations of the energy loss distribution in heavy water.

THEORY

G-values for the radiolysis of water by a variety of charged particles are now known (3). It has been observed that a definite correlation exists between the initial LET of a charged particle and the G-value resulting from its passage through water. Allen (1) has plotted the $G(Fe^{3+})$-values in the Fricke dosimeter solution as a function of the initial LET. If energy is deposited through many types of charged particles, the net G-value is a weighted sum of the G-values attributable to each type. In this section, an estimate of the G-value for fast-neutron radiolysis of heavy water is made on the basis of an analysis of the physical stage of the radiation chemical process.

Fast neutrons passing through heavy water interact with the nuclei of oxygen and deuterium. The neutron-oxygen interactions have been analyzed (6) for the case of fast-neutron radiolysis of water; the same interactions take place in heavy water. The energy transferred via the neutron-deuteron ineractions is estimated as follows.

The elastic scattering of neutrons by deuterons produces a continuous spectrum of energetic deuterons. The average energy of this spectrum can be estimated from the differential cross-section data for the elastic scattering. Figure 1, taken from reference (42), shows the differential cross-section per steradian as a function of the scattering angle in the center-of-mass system. These data are for neutrons of energy 14.1 Mev.; they are assumed to be applicable, with reasonable accuracy, to 14.6 Mev. neutrons. By applying basic principles, the energy spectrum and the

average energy of the dueterons can be evaluated from Fig. 1. The derivation of the formula used is indicated in Appendix A. The calculated differential cross-sections per unit energy for the production of deuterons of given energy are shown in Fig. 2.

As mentioned earlier, the (n,2n) reaction is represented by the equation:

$$_1H^2 + {}_0n^1 \rightarrow {}_1H^1 + 2{}_0n^1 - 2.23 \text{ Mev.}$$

On the basis of the assumptions mentioned in the "Introduction" and by the application of the principles of energy and momentum, it is found that the energy of the proton is 4.12 Mev. and the average energy of the knock-on deuterons (by elastic scattering of the neutrons from the (n,2n) reaction) is 1.83 Mev. The numerical results of the analysis of the neutron-deuteron interactions (first collision density) are listed in Table 2.

The energy loss distribution for the fast-neutron radiolysis of water, which is listed in Table 3, is computed from the information provided by Table 1 (for the neutron-oxygen interactions) and by Table 2 (for the neutron-deuteron interactions). Inspection of Table 3 shows that more than eighty-five percent of the energy lost by the neutrons is carried off by the secondary particles of the fourth, fifth and sixth interactions listed in Table 3. As a simplifying step, it is assumed that the entire amount of energy lost by the neutrons is lost via these three interactions. It is further assumed that the energy is distributed among the secondary charged particles of these interactions in the same manner as that shown in column 5 of Table 3.

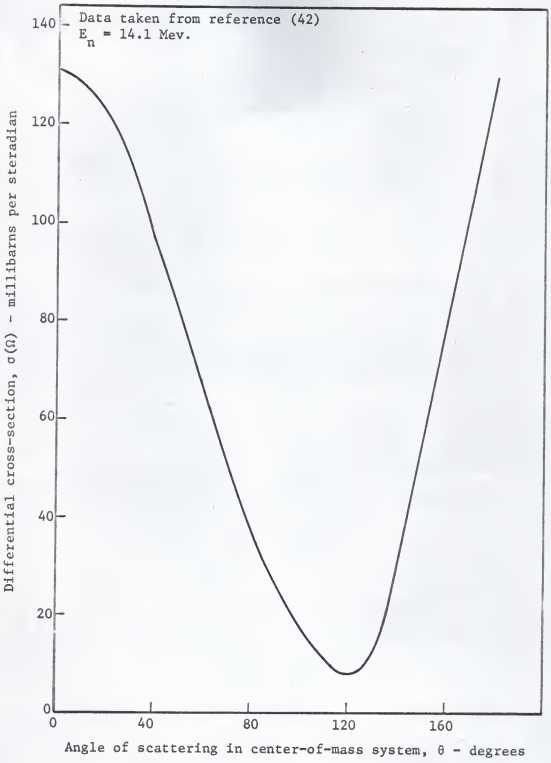

Fig. 1. Differential cross-section for n-d elastic scattering.

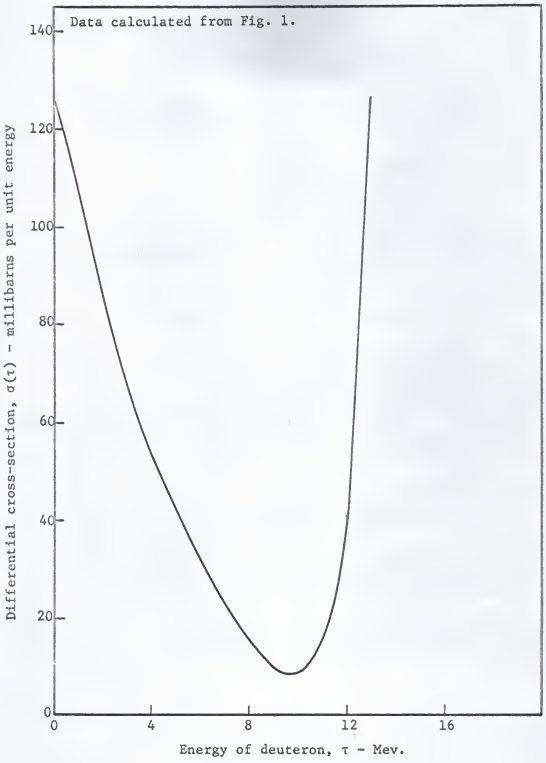

Fig. 2. Plot of $\sigma(\tau)$ vs. τ for n-d elastic scattering.

Table 2. Calculated Energy Distribution in Deuteron-Neutron Interactions[a]

1	2[b]	3[c]	4[d]	5	6[e]
Interaction , i	N'_i	σ_i	$\bar{\tau}_i$	$N'_i\sigma_i\bar{\tau}_i$	Particle
$H^2(n,n)H^2$	2/3	0.61	4.9	1.993	d
$H^2(n,2n)H^1$	2/3	0.20	4.12	0.549	p
$H^2(n,n)H^2$	38.7×10^{-3}[f]	1.87	1.83	0.133	d

[a] Refers to fast-neutron radiolysis of heavy water.

[b] N'_i is relative target nuclear density.

[c] σ_i is the cross-section for the i^{th} interaction, barns. Taken from reference (24).

[d] $\bar{\tau}_i$ is the average energy lost by the neutron, Mev.

[e] This is the significant secondary charged particle.

f See Appendix F

Table 3. Calculated Energy Distribution in Fast-Neutron Radiolysis of Heavy Water[a]

1	2[b]	3[c]	4[d]	5	6[e]	7[f]
Interaction, i	N'_i	σ_i	$\bar{\tau}_i$	$N_i\sigma_i\bar{\tau}_i$	f_i	Particle
$O^{16}(n,n)O^{16}$	1/3	0.73	0.39	0.095	0.025	O^{16}
$O^{16}(n,n')O^{16}$	1/3	0.51	1.15	0.194	0.051	O^{16}
$O^{16}(n,p)O^{16}$	1/3	0.041	4.7	0.064	0.017	p
$O^{16}(n,\alpha)C^{13}$	1/3	0.31	7.8	0.81	0.211	α
$H^2(n,n)H^2$	2/3	0.61	4.9	1.993	0.519	d
$H^2(n,2n)H^1$	2/3	0.20	4.12	0.549	0.143	p
$H^2(n,n)H^2$	38.7×10^{-3}	1.87	1.83	0.133	0.034	d

[a] Table constructed from Tables 1 and 2.

[b] N'_i is relative target nuclear density.

[c] σ_i is the cross-section for the i^{th} interaction, barns. Taken from reference (24).

[d] $\bar{\tau}_i$ is the average energy lost by the neutron, Mev.

[e] f_i is equal to $\frac{N'_i\sigma_i\bar{\tau}_i}{\sum(N'_i\sigma_i\bar{\tau}_i)}$. This is the fraction of energy deposited via the i^{th} interaction.

[f] This is the significant secondary charged particle.

On this basis, the calculated energy distribution among the secondary charged particles is listed in Table 4.

Table 4. Fractional Energy Deposition by Secondary Charged Particles

Secondary charged particle i	Average energy of the particle $\bar{\tau}_i$ Mev.	Fraction of energy deposited by particle f_i
deuteron	4.9	0.595
alpha	7.8	0.242
proton	4.12	0.163

Each of these charged particles contributes to the G-value in heavy water. The contribution of each particle depends upon the initial LET of the particle and the fraction of energy deposited by the particle. Figure 3, which is taken from reference (1) shows the variation $G(Fe^{3+})$-value with the initial LET of the ionizing radiation in light water solution. Table 5 is constructed with the aid of Table 4 and Fig. 3. This table shows that the estimated $G(Fe^{3+})$-value for the fast-neutron radiolysis of heavy water (assuming the absence of isotopic effect) is 8.45. Table 6, which is similar to Table 5, estimates the $G(Fe^{3+})$ value in light water for fast-neutron radiolysis as equal to 10.24. Therefore, the calculated ratio of the G-value in heavy water to that in light water is 0.825.

Experimental determination of G-values involves estimation of absorbed radiation dose and change in concentration of a substance from the absorb-

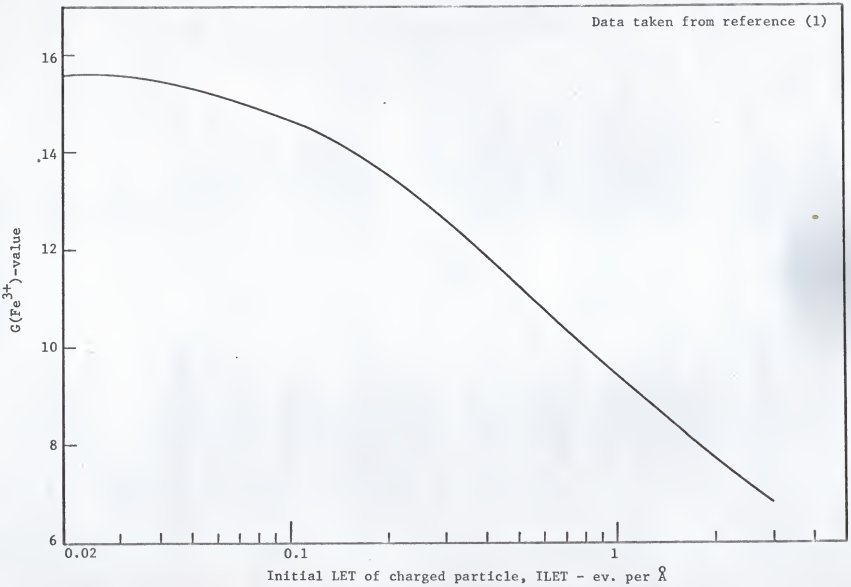

Fig. 3. Plot of $G(Fe^{3+})$ vs. ILET for Fricke dosimetric solution.

Table 5. An Estimate of $G(Fe^{3+})$-Value for Fast-Neutron Radiolysis of Heavy Water

Particle i	f_i	Initial[a] LET ILET $\frac{ev.}{A^o}$	From Fig. 3 G_i	$f_i \times G_i$
Deuteron	0.595	1.47	8.5	5.05
Alpha particle	0.242	2.04	7.7	1.86
Proton	0.163	0.99	9.4	1.54
			Total →	8.45

[a] LET data taken from reference (7).

Table 6. An Estimate of $G(Fe^{3+})$-Value for Fast-Neutron Radiolysis of Light Water

Particle i	f_i[a]	Initial[b] LET ILET $\frac{ev.}{A^o}$	From Fig. 3 G_i	$f_i \times G_i$
Proton	0.844	0.62	10.7	9.04
Alpha particle	0.156	2.04	7.7	1.20
			Total →	10.24

[a] Taken from reference (15).

[b] Taken from reference (7).

ance readings of the spectrophotometer. Absorbed dose can be evaluated by the application of the principles of radiation dosimetry. In the following discussion, based on reference (3), some definitions which are common knowledge are also included in order to insure continuity.

The exposure dose of gamma radiation, at a certain place is a measure of the ability of the radiation to produce ionization. The unit of exposure dose for gamma or X radiation is the roentgen. One roentgen is an exposure dose of gamma radiation such that the associated corpusclar emission per 0.001293 grams of air produces, in air, ions carrying one electrostatic unit of quantity of electricity of either sign.

The absorbed dose of any ionizing radiation is the energy imparted to matter by ionizing particles per unit mass of irradiated material at the place of interest. The unit of absorbed dose is the rad. One rad is equivalent to an energy absorption of 100 ergs per gram.

The absorbed dose in air exposed to gamma radiation can be calculated from the definition of the roentgen:

$$1 \text{ roentgen} = \frac{1}{0.001293} \frac{(\text{e.s.u.})}{(\text{gm.})} \times 2.082 \times 10^{9} \frac{(\text{electrons})}{(\text{e.s.u.})} \times 34 \frac{(\text{ev.})}{(\text{electron})}$$

$$\times 1.602 \times 10^{-12} \frac{(\text{ergs})}{(\text{ev.})} \times \frac{1}{100} \frac{(\text{gm. rads})}{(\text{erg})} = 0.877 \text{ rads.}$$

If the absorbed dose in air is known, the absorbed dose in any material, for the same exposure conditions, can be calculated from the equation:

$$D_m = D_a \frac{\mu_m}{\mu_a} , \qquad (1)$$

where D_m is the absorbed dose in the material; D_a is the absorbed dose in air; μ_m is the mass energy absorption coefficient of the material; and μ_a is the mass energy absorption coefficient in air.

In chemical dosimetry, the absorbed dose in a material is calculated from the known absorbed dose in the dosimetric solution by the equation:

$$D_m = D_d \frac{\mu_m}{\mu_d}, \tag{2}$$

where D_d is the absorbed dose in the dosimetric solution and μ_d is the mass energy absorption coefficient of the dosimetric solution.

Eqs. (1) and (2) are applicable for irradiation by photons. In the case of irradiation by neutrons, the ratio of the absorbed dose rates in two materials exposed to the same neutron flux is given by the equation:

$$\frac{D_1}{D_2} = \frac{(N\sigma\tau)_1}{(N\sigma\tau)_2} \times \frac{\rho_2}{\rho_1} \tag{3}$$

where D is the absorbed dose in rads; ρ is the density of the material; N is the target nuclear density; σ is the cross section for neutron interaction; and τ is the energy loss per interaction. Subscripts 1 and 2 refer to materials 1 and 2. Eq. (3) is applicable for first collision density.

For any chemical system, the G-value is given by the equation:

$$G = 100 \frac{n}{e}, \tag{4}$$

where G is the G-value of a product formed; n is the number of molecules of the product per gram of the sample irradiated; and e is the energy

absorbed in electron volts per gram of the sample irradiated. But

$$1 \frac{(\text{ev.})}{(\text{gm.})} = \frac{(\text{ev.})}{(\text{gm.})} \times 1.602 \times 10^{-12} \frac{(\text{ergs})}{(\text{ev.})} \times \frac{1}{100} \frac{\text{gm. rads}}{(\text{erg})}$$

$$= 1.602 \times 10^{-14} \text{ rads.}$$

Therefore, energy absorbed in rads = $1.602 \times 10^{-12} \frac{n}{G}$.

The number of moles formed is related to the absorbance reading of the spectrophotometer by Beer's law:

$$C = \frac{A}{\varepsilon \times L} , \tag{5}$$

where C is the number of moles of the product per liter of the sample; A is the absorbance of the sample due to the product; ε is the extinction coefficient of the product ions in the spectrophotometer; and L is the length of the optical path.

If ρ is the density of the sample, then

$$n = C \times 6.023 \times 10^{23} \times \frac{1}{1000} \times 1/\rho .$$

Therefore, D, the energy absorbed in rads = $\frac{9.65 \times 10^{8} \times A}{\varepsilon \times L \times \rho \times G}$. (6)

In this research the value of L is equal to one centimeter. Therefore, Eq. (6) simplifies to Eq. (7):

$$D = \frac{9.65 \times 10^{8} A}{\varepsilon \rho G} \tag{7}$$

Eq. (7) shows that the absorbed dose can be estimated with the aid of a spectrophotometer if G is known and vice versa.

In the fast-neutron radiolysis experiment, water and heavy water samples are exposed to the same average neutron flux and their absorbances are measured. Using Eqs. (3) and (7), it can be shown that the ratio of the G-values in heavy water and water is given by Eq. (8):

$$\frac{G_h}{G_\ell} = \frac{A_h}{A_\ell} \times \frac{\varepsilon_\ell}{\varepsilon_h} \times \frac{\sum (N_i \sigma_i \bar{\tau}_i)_\ell}{\sum (N_i \sigma_i \bar{\tau}_i)_h}, \qquad (8)$$

where the subscript i stands for the i^{th} neutron interaction; the subscript h refers to properties corresponding to heavy water; and the subscript ℓ refers to properties corresponding to light water.

DESCRIPTION OF APPARATUS

The major items of equipment used in this research were a neutron generator, a gamma irradiator and an ultraviolet spectrophotometer. This section contains brief descriptions of each item.

Neutron generator: The neutron generator serves as a source of fast neutrons needed for fast-neutron radiolysis.

There are no long-lived radioisotopes that emit neutrons directly with the exception of a few isotopes of heavy elements which undergo spontaneous fission. Neutrons can, however, be produced by stopping accelerated positive particles or high-energy electromagnetic radiation with suitable target materials.

One of the convenient nuclear reactions yielding fast neutrons is the $H^3(d,n)He^4$ reaction represented by the equation:

$$_1H^2 + _1H^3 \rightarrow _0n^1 + _2He^4 + 17.6 \text{ Mev.}$$

In this reaction, tritium is the target and the deuteron is the accelerated positive particle. The energy of the resulting neutrons may be determined by applying the principles of conservation of momentum and energy. A neutron emitted in the forward direction carries away 14.7 Mev. of energy.

For deuteron bombarding energies up to 150 kev., the neutron emission is nearly isotropic. The energy of the neutron is a weak function of the angle. In this work, the neutrons are considered to be monoenergetic with

an energy of 14.6 Mev.

The yield of neutrons is a function of the energy of the incident deuteron. When thin targets are used, maximum neutron yield is obtained at a deuteron energy of 107 kev (43).

The neutron generator of Kansas State University is supplied by Texas Nuclear Corporation, and has a nominal capacity of 10^{10} neutrons per sec. The functions of the generator are production, extraction, focusing and acceleration of deuterium ions. The major components of the generator are shown schematically in Fig. 4. Positive ions produced in a radio frequency type ion source are extracted by applying a potential across the ion source bottle. The extracted ions are focused by a gap lens. Then, the ions enter the field of the accelerating tube where they can be accelerated through a potential of 150 kv. After leaving the accelerating tube, the ions drift through a potential free region until they strike the target. A high vacuum is maintained in the entire system to minimize scattering of the ion beam. Remote operating controls are located on a console. Photographs of the generator and the control console are shown in Fig. 5 and Fig. 6 respectively.

Fig. 7 shows the sample bottles and the sample holder used for irradiation. The circular sample holder revolves at a speed of 3 r.p.m. This ensures that all the samples are exposed to the same average flux.

The gamma irradiator: The gamma irradiator serves as a source of gamma rays needed for gamma radiolysis.

Within the last decade, artifical gamma-emitting radioisotopes have become available at reasonable cost. The most widely used isotope is

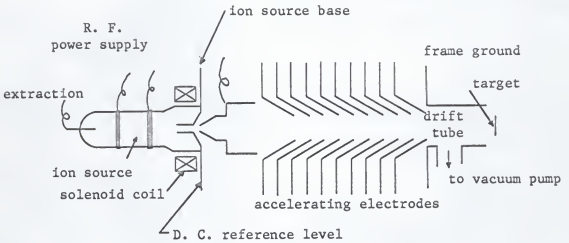

Fig. 4. Schematic diagram of the neutron generator.

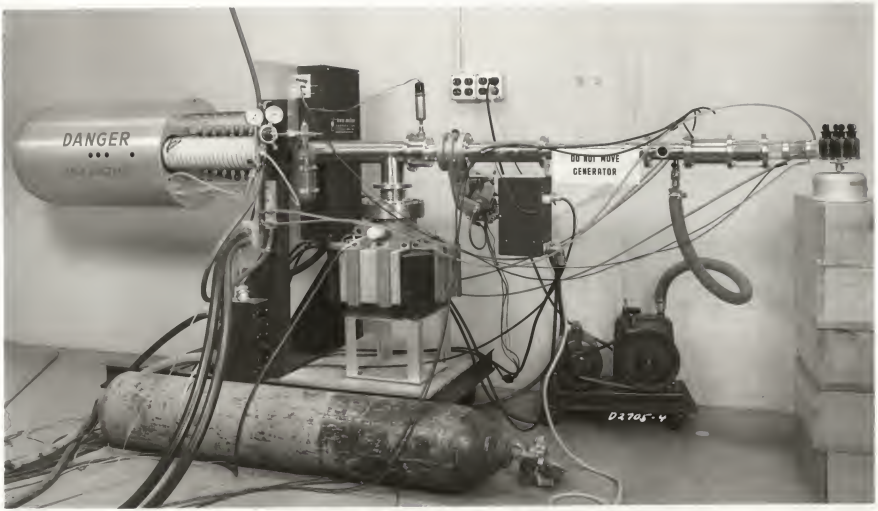

Fig. 5. A view of the neutron generator.

Fig. 6. A view of the control console of the neutron generator.


D2705-1

Fig. 7. Sample holder for fast-neutron radiolysis.

cobalt-60. Many designs are available for the source material and the associated shielding. The "Gammacell"-220 irradiator (4000 curies) of Kansas State University is supplied by the Atomic Energy of Canada, Ltd., and is shown in Fig. 8. In this design, the cobalt forms a hollow cylindrical assembly into and out of which a sample chamber can be moved. The period of irradiation can be set exactly by a timer which raises the sample chamber at the end of the pre-set time.

The ultraviolet spectrophotometer: The spectrophotometer is used to determine the concentration of ferric ions in irradiated Fricke dosimeter solutions.

Absorption spectrophotometry is based on the observation and comparison of absorption spectra. The absorption spectrum is a characteristic property of the chemical absorbing radiant energy.

Transmittance is defined as the ratio of the energy transmitted by the sample to the energy incident upon the sample. Absorbance is defined as the negative logarithm (to base 10) of the transmittance. Quantitative spectrophotometry is based on the fact that absorbance of an absorbing material is dependent upon its concentration. If the absorbance is directly proportional to the concentration, the system is said to obey Beer's law.

The Beckman Model DU Spectrophotometer is useful in the wavelength region of 220 to 1000 millimicrons. The function of the spectrophotometer is to direct monochromatic light on a sample and to measure the amount of light transmitted by the sample. Figure 9 shows its major components in

Fig. 8. A view of the "Gammacell"-220.


Gammacell 220
CAUTION
82905-3

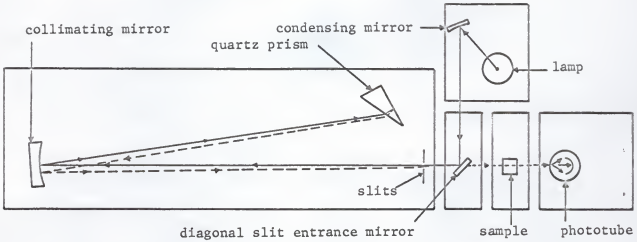

Fig. 9. Schematic diagram of the spectrophotometer.

a schematic manner.

Ferric ions, in Fricke dosimeter solutions, exhibit a maximum absorption around a wavelength of 305 mμ. A hydrogen lamp is used as the light source.

EXPERIMENTAL PROCEDURE

Three experiments leading to the determination of the $G(Fe^{3+})$-value for fast-neutron radiolysis of heavy water were performed. This section describes the procedures adopted for the experiments.

Experiments in radiation chemistry require a high degree of cleanliness in the glassware used. The procedure for cleaning the glassware is described below.

All glassware were thoroughly cleaned with the aid of a mixture of concentrated sulfuric acid and potassium permanganate. Then they were washed with tap water. This was followed by washing and rinsing with distilled water. After drying, the openings of the glassware were wrapped with paper. Sample bottles used for irradiation were subjected to further purification. Cleaned sample bottles were rinsed and filled with specially distilled water and were irradiated in the "Gammacell" for about six hours. After irradiation, they were emptied, washed with specially distilled water, dried and kept closed with stoppers.

Extremely pure water is required for the preparation of solutions which are to be irradiated. Preparation of this water (termed specially distilled water in this thesis) is described below.

The starting material was distilled water made in a Barnstead still. To this water, small quantities of potassium permanganate and potassium hydroxide were added. The water was distilled in a laboratory still fitted with a reflux condenser. The distillate was redistilled in presence of small quantities of potassium permanganate and potassium bisul-

fate. The distillate - specially distilled water - was stored in a well stoppered bottle. This water was always prepared a few hours before it was needed.

The experiments performed were: a) determination of the extinction coefficient for ferric ions in water; b) determination of the G-value of ferric ions in the gamma radiolysis of heavy water; c) determination of the G-value of ferric ions in the fast-neutron radiolysis of heavy water. The experimental procedures are described below.

a) Determination of the extinction coefficient for ferric ions in water: A set of solutions of known ferric ion concentrations were prepared, and their absorbances were measured in the spectrophotometer. The set of standard ferric solutions were prepared by mixing, in varying proportions, a parent ferric solution with a blank solution. The preparation of these two solutions are described below.

Parent ferric solution: The following chemicals were used:

Pure iron wire:	99.89 % Fe.
6 normal hydrochloric acid:	Made by mixing reagent grade hydrochloric acid with distilled water.
Ammonium persulfate:	Reagent grade.
95-98 % sulfuric acid:	Reagent grade.
Distilled water:	Made in Barnstead still.

About 0.06 grams of the iron wire were weighed accurately in an electronic balance and allowed to dissolve in 20 ml. of the hydrochloric acid. About 2 grams of the ammonium persulfate were added and the solution was

warmed. Then the solution was transferred to a 1000 ml. volumetric flask to which 22 ml. of the sulfuric acid were added. The solution was made up to 1000 ml. with the distilled water.

Blank solution: All the chemicals excepting the iron wire, used in the preparation of the parent ferric solution, were used. The blank solution was prepared exactly in the same manner as the parent ferric solution was.

The parent ferric solution was about 10^{-3} molar with respect to ferric iron. A set of solutions in the range of 10^{-4} molar (ferric) was made by dilution of this solution with the blank solution.

The absorbances of these solutions were determined by comparing the amount of light transmitted by each solution with that transmitted by the blank solution. The blank solution was placed in one of the optical cells of the spectrophotometer. The ferric solution of known strength was placed in another cell. Both the cells were placed in the cell compartment of the spectrophotometer. The blank solution was brought into the optical path and the needle of the null meter was zeroed with the aid of the sensitivity control, the selector switch being in the "check" position. Next, the ferric solution was brought into the optical path, and the null meter was zeroed with the aid of the transmittance knob, the selector switch being in the "1" position. The reading on the absorbance scale and the temperature of the solution were noted. This procedure was repeated for each ferric solution.

The procedural details for the use of the spectrophotometer are given

in reference (9). Measurements were taken at a wavelength of 305 mμ and with a slit width of 0.1 mm. The cell compartment was kept at a temperature of 23°-25°C by circulating cooling water.

b) Determination of the G-value of Fe^{3+} in gamma radiolysis of heavy water: The experiment consisted of four stages: i) preparation of Fricke dosimeter solution in light water, ii) preparation of dosimeter solution in heavy water, iii) irradiation of light water dosimeter solution and measurement of its absorbance and iv) irradiation of heavy water dosimeter solution and measurement of its absorbance. The procedures are given below.

i) Preparation of Fricke dosimeter solution in light water: This was prepared according to the recipe given in reference (46). The following chemicals were used:

Ferrous ammonium sulfate ($Fe(NH_4)_2(SO_4)_2 \cdot 6H_2O$): Reagent grade.
Sodium chloride: Reagent grade.
95-98 % sulfuric acid: Reagent grade.
Specially distilled water: Prepared as described earlier.

0.4 grams of the ferrous ammonium sulfate, 0.06 grams of the sodium chloride and 22 ml. of the sulfuric acid were dissolved in the distilled water and the solution was made up to a liter with the distilled water. The solution was stored, away from sunlight, in an amber colored bottle.

ii) Preparation of dosimeter solution in heavy water: This solution was prepared in the manner described under (i) with the variation that 99.5 percent heavy water (purchased from Matheson Coleman and Bell) was used in place of the specially distilled

water.

iii) Irradiation of dosimeter solution in light water (i) and measurement of absorbance: A pre-irradiated sample bottle was filled with the solution and placed in the sample chamber of the "Gamma-cell". A sample holder, to make the center of the bottle coincide with the center of the sample chamber, was used. The sample was irradiated for three minutes. Its absorbance was measured by comparison with a non-irradiated sample of the solution. The nominal absorbed dose was 10^4 rads.

iv) Irradiation of dosimeter solution in heavy water (ii) and measurement of absorbance: The procedure adopted was exactly the same as that adopted in (iii).

c) Determination of the G-value of Fe^{3+} in fast-neutron radiolysis of heavy water: Dosimeter solutions in light water (b-i) and heavy water (b-ii) were irradiated simultaneously under identical conditions by the neutron generator. Identical conditions of irradiation were ensured by placing the bottles on a revolving sample holder (Fig. 7) and keeping them as close to the target as possible. After irradiation for eight hours, the absorbances of the samples were compared with those of the corresponding non-irradiated samples. In each run, three samples of light water and three samples of heavy water were irradiated. The nominal absorbed dose was 200 rads. Operating instructions for the neutron generator are given in reference (44).

PRESENTATION OF DATA AND DATA ANALYSIS

The data collected from the experiments were analyzed to arrive at the results: a) best value of the extinction coefficient for Fe^{3+} ions in the Fricke dosimetric solution; b) the ratio of the $G(Fe^{3+})$-values in heavy water and light water solutions for cobalt-60 gamma radiolysis; and c) best value of the ratio of absorbances of heavy water and light water for fast-neutron (14.6 Mev.) radiolysis.

a) Extinction Coefficient for Fe^{3+} Ions in the Fricke Dosimetric Solution

Table 7 lists the absorbances of the standard ferric solutions as measured in the spectrophotometer. The variation of absorbance with con-

Table 7. Absorbances of Standard Ferric Solutions[a]

No. i	Concentration of solution moles (Fe^{3+})/liter C_i	Absorbance of solution A_i
1	5.981×10^{-4}	1.232
2	2.991×10^{-4}	0.634
3	2.617×10^{-4}	0.547
4	2.243×10^{-4}	0.468
5	1.869×10^{-4}	0.387
6	1.495×10^{-4}	0.316
7	1.197×10^{-4}	0.262

[a] Temperature...24°C; wave length...305 mμ; slit width...0.1 mm.; instrument model...Beckman DU Model 2400.

centration is shown in Fig. 10. This straight line plot shows that in the concentration range represented by the points 2 through 7, the absorbance of a solution is predictable by Beer's law. The scatter of point 1 shows that deviations from Beer's law occur as the concentration is increased. Such deviations are caused by one or more effects coming into play at higher concentrations. Hydrogen bonding, ion pair formation, solvation and other physical or chemical interactions alter the simple relationship between the absorbance and the concentration of a solution.

According to Beer's law, the extinction coefficient is given by Eq. (5):

$$C = \frac{A}{\epsilon \times L} . \qquad (5)$$

In this experiment L was equal to one centimeter. A best value for the extinction coefficient was calculated by a least squares analysis of the data points 2 through 7. The method is indicated in Appendix B. The best value for the extinction coefficient was found to be equal to $2103 \pm 27 \frac{\text{liters}}{\text{mole. cm.}}$ at $24^{\circ}C$.

The extinction coefficient has a temperature coefficient of + 0.7 percent per degree centigrade (19, 20). It also depends to some extent on the particular instrument used.

The value for the extinction coefficient of Fe^{3+} ions in heavy water solutions was calculated from the published value (31) of the ratio of the extinction coefficients in heavy water and light water solutions. This ratio is equal to 1.068 ± 0.004 at $25^{\circ}C$ (A Carey recording spectrophotometer was used for this experiment. No information as to how the error was estimated is available).

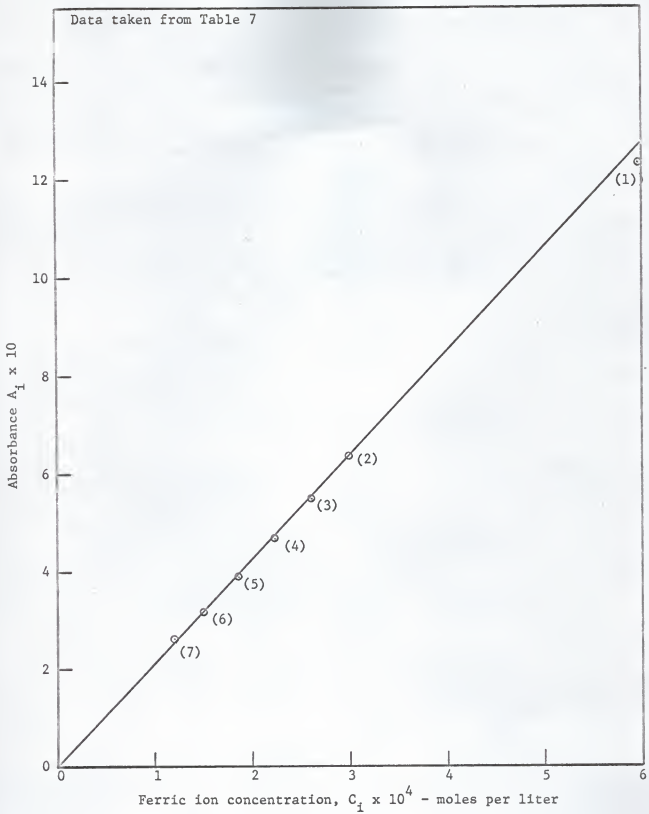

Fig. 10. Plot of absorbance vs. ferric ion concentration.

b) The Ratio of the $G(Fe^{3+})$-Values in Heavy Water and Light Water Solutions for Cobalt-60 Gamma Radiolysis

The raw data of absorbances of the irradiated solutions of light water and heavy water are listed in Tables C-1 and C-2 respectively in Appendix C. The mean value of the absorbance of the light water solution was 0.4466 while the corresponding figure for the heavy water solution was 0.4922.

The absorbed dose in light water solution was calculated with the aid of Eq. (7), using a value of 15.5 for G. The absorbed dose in air was calculated using Eq. (1). The exposure dose in air was obtained by dividing the absorbed dose in air by 0.877. The absorbed dose in heavy water was calculated again using Eq. (1). From the measured absorbance and the calculated absorbed dose, the G-value was calculated using Eq. (7). The numerical calculations are given in Appendix C.

The $G(Fe^{3+})$-value for gamma radiolysis of heavy water was found to be equal to 16.76 and the ratio of the G-values in heavy water and light water solutions was found to be equal to 1.084. Since only two runs were made with heavy water, no error analysis is presented.

c) Ratio of Absorbances of Heavy Water and Light Water for Fast-Neutron (14.6 Mev.) Radiolysis

The raw data of absorbances of light water and heavy water are presented in Table D-1 of Appendix D. These data were subjected to a statistical analysis to find the best values of absorbances for each run. A sample calculation of this analysis is presented in Appendix E. Table 8 lists the best values of the absorbances of light water and heavy water and the ratio of the absorbances $(\frac{A_h}{A_l})_i$. Run 2 was abandoned owing to unsatis-

factory operating conditions of the neutron generator. The spread in the values of $(\frac{A_h}{A_\ell})_i$ is probably due to the absorbance readings falling in a range which is far from the optimum reading range of the spectrophotometer.

Table 8. Absorbances in Fast-Neutron Radiolysis[a]

Run No. i	Mean absorbance in light water $(A_\ell)_i$	Mean absorbance in heavy water $(A_h)_i$	Ratio of mean absorbances $(\frac{A_h}{A_\ell})_i$
1	0.0435 ± 5.3 %	0.0437 ± 4.6 %	1.005 ± 9.9 %
3	0.0484 ± 1.7 %	0.0466 ± 1.1 %	0.963 ± 2.8 %
4	0.0564 ± 2.0 %	0.0578 ± 1.7 %	1.03 ± 3.7 %
5	0.0723 ± 1.4 %	0.0684 ± 1.5 %	0.946 ± 2.9 %
6	0.0591 ± 1.5 %	0.0572 ± 2.6 %	0.968 ± 4.1 %

[a] Obtained from raw data (Appendix D) and statistical analysis (Appendix E).

The best value, $\frac{A_h}{A_\ell}$, was calculated by the method of weighting the $(\frac{A_h}{A_\ell})_i$ values with their variances (2). Thus, $\frac{A_h}{A_\ell}$ is given by the equation:

$$\frac{A_h}{A_\ell} = \frac{\sum \frac{1}{\bar{\sigma}_i^2} (\frac{A_h}{A_\ell})_i}{\sum (\frac{1}{\bar{\sigma}_i^2})}$$

where $\bar{\sigma}_i^2$ is the variance of $(\frac{A_h}{A_\ell})_i$. The variance of the best value is equal to $\frac{1}{\sum \frac{1}{\bar{\sigma}_i^2}}$. Using the appropriate "t" value for the 95 % confidence limit,

the value of $\frac{A_h}{A_\ell}$ was found to be 0.970 ± 0.0432 (i.e. for 95 % confidence). The results of the experiment are discussed in the following section.

RESULTS AND CONCLUSIONS

a. Extinction Coefficient of Fe^{3+} Ions in 0.8 N H_2SO_4 Solution

Table 9 lists the values of the extinction coefficient determined in other laboratories along with the value obtained in this research corrected to 25°C.

Table 9. Comparison of the Values of the Extinction Coefficient for Fe^{3+} in 0.8 N H_2SO_4 at 25°C (1)

Source	Value of extinction coefficient
Argonne National Laboratory	2225
Brookhaven National Laboratory	2195
Cambridge University	2161
This Research	2118

The result obtained in this research is slightly lower than the values with which it is compared. As stated earlier the value depends to some extent on the particular instrument used. The wavelength at which the absorption by ferric ions is greatest is in the range of 302-305 mμ depending upon the instrument calibration. Wavelength calibration was not performed in this research. Experimentally determined G-values in this research do not depend upon the absolute value of the above extinction coefficient.

As stated earlier this extinction coefficient has a large temperature

coefficient. According to Hochanadel and Ghormley (21) the extinction coefficient at 275 mμ is almost independent of temperature and its value is 1830. A low value of extinction coefficient necessitates longer irradiation periods; hence this wavelength is not very attractive.

Scharf and Lee (41) have recommended making measurements at 224 mμ. The value of the extinction coefficient at this wavelength is 4565, enabling smaller doses to be measured. The temperature coefficient is smaller too (+ 0.1%). However, in the model DU spectrophorometer used in this research, this could be achieved only with very high sensitivity settings leading to undesirable amount of fluctuations of the needle of the null meter.

b. Ratio of $G(Fe^{3+})$-Values in Heavy Water and Light Water for Cobalt-60 Gamma Radiolysis

Table 10 lists the values of this ratio determined by other workers along with the one obtained in this research.

Table 10. Comparison of the Ratio of G-Values for Gamma Radiolysis

Source	Ratio $\frac{G_h}{G_\ell}$
Hardwick (17)	1.093
Mahlman and Boyle (30)	1.072
This Research	1.084

Table 10 shows that the result obtained in this research compares favorably with others, indicating that the experimental techniques adopted were satisfactory. The divergence of $\frac{G_h}{G_\ell}$ from unity has been tentatively attributed to the longer dielectric relaxation time in D_2O than in H_2O which might allow the electron to diffuse further from the track, leading to a broader distribution of D atoms in D_2O than of H atoms in H_2O. Another possible cause may be that the extent of recombination reaction, $D + OD \rightarrow D_2O$, in D_2O may be less than the extent of the reaction $H + OH \rightarrow H_2O$ in H_2O.

The experimental techniques are simplified to some extent by the flexibility offered by the Fricke dosimetric solution. The presence of a small amount of chloride in the dosimetric solution inhibits the oxidation of ferrous ions by traces of organic impurities because halide ions can enter into rapid electron transfer reactions (3) with hydroxyl radicals as represented by the equation:

$$OH^{\cdot} + C\ell^{-} + H^{+} \rightarrow C\ell^{\cdot} + H_2O.$$

The chloride oxidizes one ferrous ion just as the $OH^{\cdot}$ radical would have in the absence of organic impurities:

$$C\ell^{\cdot} + Fe^{2+} \rightarrow Fe^{3+} + C\ell^{-}.$$

The addition of chloride is unnecessary if both the water and the reagents used are purified exhaustively.

The response of the Fricke dosimeter is independent of the dose rate

up to about 10^7 rads per second (36, 4). The response is independent of the ferrous ion concentration between 5×10^{-2} and 10^{-4} molar (47, 21) and of sulfuric acid concentration between 1.5 and 0.1 N (13). However, these concentrations have to be kept at the same values for all the experiments because the density, the energy absorption coefficient and the extinction coefficient are affected by these concentrations.

The yield of the dosimeter is not significantly affected by the temperature of the solution during irradiation in the range of temperatures from 0° to 65°C (21, 40).

Many types of chemical dosimeters have been developed (3). The Fricke dosimeter was used in this research because it has been extensively used and the response found to be reproducible. Axtmann and Licari (6) think that more sensitive chemical dosimeters- i.e., the quinine dosimeter proposed by Barr and Stark (8), might serve better especially at very low dose rates.

c. The Ratio of $G(Fe^{3+})$-Values in Heavy Water and Light Water for Fast-Neutron Radiolysis.

The result of the fast-neutron radiolysis experiment was presented as the ratio of the absorbances, $\frac{A_h}{A_\ell}$, because of the uncertainties in cross-sections for the neutron interactions and in the calculations of energy loss distribution (Table 2). Axtmann and Licari (6) estimate a 10% uncertainty in the cross-sections for neutron interactions in light water. A 10% uncertainty in the cross-sections for neutron interactions in heavy

water is assumed. The ratio

$$\frac{\sum (N_i \sigma_i \bar{\tau}_i)_\ell}{\sum (N_i \sigma_i \bar{\tau}_i)_h}$$

can be written in the form:

$$\frac{\sum (N_i \sigma_i \bar{\tau}_i)_\ell}{\sum (N_i \sigma_i \bar{\tau}_i)_h} = \frac{\sum (N_i \sigma_i \bar{\tau}_i)_{\ell O} + \sum (N_i \sigma_i \bar{\tau}_i)_{\ell H}}{\sum (N_i \sigma_i \bar{\tau}_i)_{hO} + \sum (N_i \sigma_i \bar{\tau}_i)_{hD}}$$

where $(N_i \sigma_i \bar{\tau}_i)_{\ell O}$ represents neutron interactions with the oxygen nuclei in water;

$(N_i \sigma_i \bar{\tau}_i)_{\ell H}$ represents neutron interactions with the hydrogen nuclei in water;

$(N_i \sigma_i \bar{\tau}_i)_{hO}$ represents neutron interactions with the oxygen nuclei in heavy water; and

$(N_i \sigma_i \bar{\tau}_i)_{hD}$ represents neutron interactions with the deuterium nuclei in heavy water.

Using this form, it can be shown that the relative uncertainty in the quantity

$$\frac{\sum (N_i \sigma_i \bar{\tau}_i)_\ell}{\sum (N_i \sigma_i \bar{\tau}_i)_h}$$

is 4.2%. The ratio of the G-values is given by Eq. (8):

$$\frac{G_h}{G_\ell} = \left(\frac{A_h}{A_\ell}\right) \times \left(\frac{\varepsilon_\ell}{\varepsilon_h}\right) \times \frac{\sum (N_i \sigma_i \bar{\tau}_i)_\ell}{\sum (N_i \sigma_i \bar{\tau}_i)_h} . \qquad (8)$$

Using the experimentally determined value of $\frac{A_h}{A_\ell}$ and neglecting the uncertainty in the ratio $\frac{\epsilon_\ell}{\epsilon_h}$, the value of $\frac{G_h}{G_\ell}$ turns out to be 1.059 ± 0.092 The theoretically estimated value of the ratio, assuming the absence of the isotopic effect, is 0.825. The fast-neutron radiolysis experiment has not been performed by others. Hence, a comparison of results is not possible.

The fairly low amount of scatter in the raw data (Appendix D) shows that all the samples were exposed to the same average neutron flux. The only drawback of this experiment was the relatively low absorbed dose ($\sim$ 300 rads) leading to low absorbance readings in the spectrophotometer. It was not possible to increase the dose rate because the shielding of the neutron generator is not adequate to permit larger fluxes. The duration of irradiation was eight hours and nothing substantial can be gained by increasing this period because the life of the tritium target used falls exponentially with time. Instead of the six samples used, had only one sample been irradiated by tying it to the target, the absorbed dose would have been much higher. However, the neutron flux will have to be measured by some other method and it is believed that the final results will not be better than what have been obtained.

The lower limit to the absorbed dose in the Fricke dosimeter is the dose that produces sufficient ferric ion concentration to be accurately measured. Even though low absorbances can be measured by taking sufficient care, the desirable absorbance range is around 0.5 for a photoemissive noise-limited type spectrophotometer. Theoretically speaking, the absor-

bance readings can be shifted either by altering the cell thickness (L) or by inserting a filter in the optical path.

Low absorbed doses can be satisfactorily measured by increasing the sensitivity of the analytical method. In the photometric method, this can be achieved by making a derivative of ferric ion that has a higher extinction coefficient than the ferric ion. Ehrenberg and Saeland (14) used the thiocyanate complex (ε = 8500 at 465 mμ). The convenience aspect of this method has to be studied. Rudstam and Svedberg (37) were able to measure doses of 1 to 100 rads to better than 2 rads by adding Fe^{59} to the dosimeter solution as a radioactive tracer and subsequently isolating and counting the ferric ions formed. This method seems to be attractive but needs careful calibration and standardization of techniques.

Another way of overcoming the problem of low absorbed dose is to employ sensitive dosimeters. Reference (3) gives a comparative study of the chemical dosimeters. The aqueous quinine sulfate system (as mentioned earlier) and the aqueous calcium benzoate system (3) bid fair to be useful as dosimeters for low doses. Fluorescence detectors have to be employed for measuing the absorbed dose with these dosimeters.

The isotopic effect in heavy water is at present being studied by many scientists. In this thesis, no attempt is made to deal with this topic (though it is mentioned frequently!) because of the following reasons:

a) Physical properties like dielectric constant, diffusion rates and reaction rates are not known to the extent of certainty desired;

b) The identity of species formed during the physical and physico-chemical stage of the radiation-chemical process is not established

beyond doubt; and

c) the accuracy of dosimetric methods is subject to further improvement.

The rather large discrepancy between the predicted and experimentally determined values of the ratio $\frac{G_h}{G_\ell}$ remains to be explained. The isotopic effect is expected to increase the predicted value and thus reduce the discrepancy. There is an uncertainty in the calculations of energy loss distribution in heavy water due to the reasons stated in the "Introduction". It is believed that the average energy of the secondary protons created in the (n,2n) reaction may be higher than 4.12 Mev. (Table 2). If this turns out to be the case, then the experimental values of $\frac{G_h}{G_\ell}$ will be decreased and the predicted value will be increased, again reducing the discrepancy.

The cause of the isotopic effect is not known clearly at present. It may turn out that the shape of the curve in Fig. 3 may be quite different for the case of heavy water, particularly in the case of densely ionizing radiation. In stating this, the writer is merely hinting at a possibility.

ACKNOWLEDGEMENT

The writer takes this opportunity to express his deep sense of gratitude to Dr. Richard E. Faw for his guidance, encouragement and extremely helpful attitude throughout the course of this work. Sincere thanks are also offered to Dr. W. R. Kimel for his interest and kindness, to Mr. K. A. Watts for his assistance in construction of the apparatus and to Mrs. Joan Hart for typing the thesis and for her invaluable editorial assistance. The writer expresses his sincere appreciation to the United States Department of State and the Agency for International Development for supporting his studies at Kansas State University.

REFERENCES

General References

1. Allen, A. O.
The Radiation Chemistry of Water and Aqueous Solutions, Van Nostrand, N. J. (1961).

2. Mickley, H. S., T. K. Sherwood and C. E. Reed
Applied Mathematics in Chemical Engineering, McGraw-Hill, N. Y. (1957).

3. Spinks, J.W.T. and R. J. Woods
An Introduction to Radiation Chemistry, John Wiley, N. Y. (1964).

Specific References

4. Anderson, A. R.
J. Phys. Chem., 66, 180 (1962).

5. Armstrong, W. A. and W. G. Humphreys
Can. J. Chem., 42, 1092-96 (1964).

6. Axtmann, R. C. and J. A. Licari
Radiation Research, 22, 511-18 (1964).

7. Barkas, W. H. and M. J. Berker
Tables of Energy Losses and Ranges of Heavy Charged Particles, NASA SP-3013, Washington, D. C. (1964).

8. Barr, N. F. and M. B. Stark
Radiation Research, 9, 89 (1958).

9. Beckman Instruments Inc.
Instruction Manual 305-A for Model DU Spectrophotometer.

10. Bethe, H. A. and J. Ashkin
Experimental Nuclear Physics (Ed. Segre, E.) Vol. 1, p. 166, John Wiley, N. Y. (1953).

11. Cerineo, et al.
Phys. Rev., 133, 959 (1964).

12. Debertin, K., K. Hofmann and E. Rossle
Nucl. Phys., 81, 220-24 (1966).

13. Dewhurst, H. A.
Trans. Faraday Soc., 49, 1174 (1953).

14. Ehrenberg, L. and E. Saeland
JENER Publications, 8 (1954).

15. Faw, R. E.
Charged Particle Slowing-Down Spectra and Energy Loss Distribution for Fast-Neutron Irradiation of Water (to be published).

16. Ghormley, J. A.
Radiation Chemistry of Gases (Ed. Lind, S. C.) p. 59, Reinhold, N. Y. (1961).

17. Hardwick, T. J.
J. Chem. Phys., 31, 226 (1959).

18. Hart, E. J.
Ann. Rev. Nucl. Sci., 15, 125-50 (1965).

19. Haybittle, J. L., R. D. Saunders and A. J. Swallow
J. Chem. Phys., 25, 1213 (1956).

20. Henderson, C. M. and N. Miller
Radiation Research, 13, 641 (1960).

21. Hochanadel, C. J. and J. A. Ghormley
J. Chem. Phys., 21, 880 (1953).

22. Ilakovac, K., et al.
Phys. Rev. Lett., 6, 356 (1961).

23. Ilakovac, K., et al.
Nucl. Phys., 43, 254 (1963).

24. Kalos, M. H., H. Goldstein and J. Ray
Revised Cross-Sections for Neutron Interactions with Oxygen and Deuterium, UNC-5038 (1962).

25. Koehler, D. R. and R. A. Mann
Phys. Rev., 135, B91 (1964).

26. Kupperman, A. and G. Belford
J. Chem. Phys., 36, p. 1412 (1962).

27. Kupperman, A.
J. Chem. Educ., 36, 279-85 (1959).

28. Lazo, R. M., H. A. Dewhurst and M. Burton
J. Chem. Phys., 22, 1370 (1954).

29. Lind, S. C.
Am. Chem. J., 47, 397 (1912).

30. Mahlman, H. A. and J. W. Boyle
J. Am. Chem. Soc., 80, 773 (1958).

31. Mahlman, H. A. and J. W. Boyle
Radiation Research, 16, 416-21 (1962).

32. Platzman, R. L.
Radiation Biology and Medicine (E. Claus, W. D.), p. 15-72, Addison-Wesley, N. Y. (1958).

33. Platzman, R. L.
Radiation Research, 2, 1 (1955).

34. Platzman, R. L.
Basic Mechanisms in Radiobiology, Nat. Res. Council Publication 305, Washington, D. C. (1953).

35. Rossi, B.
High-Energy Particles, Prentice-Hall, N. J. (1952).

36. Rotblat, J. and H. C. Sutton
Proc. Roy. Soc. (London), Ser. A, 255, 490 (1962).

37. Rudstam, G. and T. Svedberg
Nature, 171, 648 (1953).

38. Samuel, A. H. and J. L. Magee
J. Chem. Phys., 21, 1080 (1953).

39. Schwarz, H. A.
Radiation Research Supplement, 4, 89 (1964).

40. Schwarz, H. A.
J. Am. Chem. Soc., 76, 1587 (1954).

41. Scharf, K. and R. M. Lee
Radiation Research, 16, 115 (1962).

42. Seagrave, J. D.
Phys. Rev., 97, 757 (1955).

43. Texas Nuclear Corporation
Texas Nuclear Corporation Neutron Generators.

44. Texas Nuclear Corporation
Operation Manual for Pulse Neutron Generator.

45. Trumbore and Aten
J. Am. Chem. Soc., 78, 4179 (1956).

46. Weiss, J., A. O. Allen and H. A. Schwarz
Proc. Intern. Conf. Peaceful Uses Atomic Energy, United Nations, 14, 179 (1956).

47. Weiss, J.
Nucleonics, 10, (July), 28 (1962).

APPENDIX A

Average Energy of the Deuteron Source Spectrum

The differential cross-section (for elastic scattering) per unit energy is related to the differential cross-section per steradian by the equation:

$$\sigma(\tau)\, d\tau = \sigma(\Omega)\, d\Omega. \tag{A-1}$$

where $\sigma(\tau)$ is the differential cross-section per unit energy for an energy loss τ and $\sigma(\Omega)$ is the differential cross-section per steradian for scattering in the direction Ω. (It is stipulated that $d\tau$ in energy corresponds to $d\Omega$ in direction for elastic scattering.)

For azimuthally symmetric scattering, $d\Omega$ is given by the equation:

$$d\Omega = 2\pi \sin\theta\, d\theta, \tag{A-2}$$

where θ is the angle of scattering in the center-of-mass system. The energy loss, τ, is related to the angle of scattering by the equation (based on conservation laws):

$$\tau = E_n \frac{2M}{(M+1)^2}(1 - \cos\theta). \tag{A-3}$$

where E_n is the energy of the incident neutron and M is the mass of the target nucleus (deuteron). Hence

$$d\tau = E_n \frac{2M}{(M+1)^2} \sin\theta\, d\theta. \tag{A-4}$$

Substituting Eq. (A-2) and Eq. (A-4) in Eq. (A-1),

$$\sigma(\tau) = \sigma(\Omega) \left[\frac{2\pi}{E_n} \frac{(M + 1)^2}{2M} \right]. \qquad \text{(A-5)}$$

Here

$$E_n = 14.6 \text{ Mev.} \quad \text{and} \quad M = 2;$$

therefore

$$\sigma(\tau) = \frac{\sigma(\Omega) \times 2\pi \times 9}{14.6 \times 4}$$

and

$$\tau = 14.6 \times \frac{4}{9} (1 - \cos\theta).$$

Using the above relationships and the data in Fig. 1, $\sigma(\tau)$ can be plotted as a function of τ.

The average energy loss is given by the equation:

$$\bar{\tau} = \frac{\int \tau\sigma(\tau)\, d\tau}{\int \sigma(\tau)\, d\tau}. \qquad \text{(A-6)}$$

$\bar{\tau}$ is evaluated by graphical integration. The limits of integration (based on conservation laws) are $\tau_{min.}$ and $\tau_{max.}$, where $\tau_{min.}$ is equal to zero and $\tau_{max.}$ equals $\frac{4M}{(M + 1)^2} E_n$.

The value of $\bar{\tau}$ works out to be 4.9 ± 0.1 Mev.

APPENDIX B

Determination of a Best Value of the Extinction Coefficient

A best value for the extinction coefficient is arrived at by applying the method of least squares. In the following discussion, standard matrix notation is used to represent the sets of absorbances and concentrations.

The concentration, C, and the absorbance, A, are related by Beer's law:

$$\varepsilon \{C\} = \{A\} , \tag{B-1}$$

for unit cell thickness. If $\{r\}$ is the experimental error, Eq. (B-1) becomes:

$$\varepsilon\{C\} = \{A\} + \{r\} . \tag{B-2}$$

If R is the magnitude of the sum of the squares of the errors, R is given by the equation:

$$R = [r]\{r\} = (\varepsilon\{C\} - \{A\})^T(\varepsilon\{C\} - \{A\}). \tag{B-3}$$

Postulating that R should be a minimum, the best value of ε is given by the equation:

$$\varepsilon[C]\ \{C\} = [A]\{C\} . \tag{B-4}$$

Therefore, the best value,

$$\varepsilon = \frac{\sum(A_i C_i)}{\sum(C_i^2)} . \tag{B-5}$$

The error in this value can be shown to be equal to $\frac{\sqrt{R}}{\sqrt{\sum(c_i^2)}}$. Thus, the calculated value of ε is $2103 \pm 27 \frac{\text{liters}}{(\text{mole})(\text{cm.})}$.

APPENDIX C

Raw Data and Calculations of Gamma Radiolysis

Table C-1. Absorbance in Fricke Dosimeter Solution on Gamma Radiolysis[a]

Run no. i	Trial no. k	Absorbance readings A_{ik}	Mean of absorbance readings A_i	Mean absorbance A_ℓ
1	1	0.448	0.4473	
	2	0.448		
	3	0.446		
2	1	0.446	0.4463	
	2	0.446		
	3	0.447		
				0.4466
3	1	0.447	0.4467	
	2	0.446		
	3	0.447		
4	1	0.447	0.4463	
	2	0.446		
	3	0.446		

[a] Temperature...23°C, wavelength...305 mμ, slit width...0.1 mm., date...2-7-66.

Table C-2. Absorbance in Heavy Water Solution on Gamma Radiolysis[a]

Run no. i	Trial no. k	Absorbance readings A_{ik}	Mean of absorbance readings A_i	Mean absorbance A_h
	1	0.500[b]		
1	2	0.492	0.492	
	3	0.492		
				0.4922
	1	0.496[b]		
2	2	0.493	0.4925	
	3	0.492		

[a] Temperature...25°C, wavelength...305 mμ, slit width...0.1 mm., date 6-16-66.

[b] Data rejected.

Calculations

Exposure dose rate of the "Gammacell". Mean value of the absorbance of the light water solution = 0.4466.

Temperature of absorbance measurement = 23°C.

Extinction coefficient for Fe^{3+} ions at 23°C = 2088 liters/mole cm.

Density of the solution = 1.024 gm./cm.^{3}.

$G(Fe^{3+})$-value of the solution = 15.5.

Absorbed dose in the solution (from Eq.(7)) $= \frac{9.65 \times 10^8 \times 0.4466}{2088 \times 1.024 \times 1 \times 15.5}$

= 13,000 rads.

Absorbed dose in air (from Eq.(1)) $= 13{,}000 \times \frac{0.499}{0.553} = 11{,}730$ rads.

Exposure dose in air $= 11{,}730 \times \frac{1}{0.877} = 13{,}380$ roentgens.

Duration of irradiation = 3 mins.

Exposure dose rate $= 13{,}380 \times \frac{60}{3} = 2.676 \times 10^5$ roentgens per hour.

The exposure dose rate of the "Gammacell" decreases exponentially with time; the decay constant of cobalt-60 is 0.01096 month^{-1}.

(Fe^{3+})-value of heavy water. Mean value of the absorbance of the heavy water solution = 0.4922.

Temperature of absorbance measurement = $25^{\circ}C$.

Extinction coefficient of Fe^{3+} ions in the heavy water solution = 2262 $\frac{\text{liters}}{\text{mole cm.}}$.

Density of the heavy water solution = 1.117 gm./cm.^3.

Exposure dose rate on the day of measurement (calculated) $= 2.553 \times 10^5$ roentgens per hour.

Absorbed dose rate in air $= 2.553 \times 10^5 \times 0.877 = 2.239 \times 10^5$ rads per hour.

Absorbed dose rate in solution (from Eq. (1)) $= 2.239 \times 10^5 \times \frac{0.500}{0.499} = 2.244 \times 10^5$ rads per hour.

Duration of irradiation = 3 minutes.

Absorbed dose in solution $= 2.24 \times 10^5 \times \frac{3}{60} = 1.122 \times 10^4$ rads.

$G(Fe^{3+})$-value of the heavy water solution (from Eq.(7))

$$= \frac{9.65 \times 10^8 \times 0.4922}{2262 \times 1.122 \times 10^4 \times 1.117 \times 1} = 16.76.$$

$$\frac{G(Fe^{3+})\text{-value of heavy water solution}}{G(Fe^{3+})\text{-value of light water solution}} = \frac{16.76}{15.5} = 1.084$$

APPENDIX D

Raw Data of the Fast-Neutron Radiolysis Experiment

Table D-1. Absorbance Readings in Fast-Neutron Radiolysis

Run no. i	Sample no. j	Trial no. k	Light Water Solution: Absorbance readings A_{ijk}	Light Water Solution: Mean of absorbance readings A_{ij}	Heavy Water Solution: Absorbance readings A_{ijk}	Heavy Water Solution: Mean of absorbance readings A_{ij}
1	1	1	0.042	0.042	0.048	0.0493
		2	0.042		0.048	
		3	0.042		0.052	
	2	1	0.052	0.0517	0.048	0.0457
		2	0.052		0.045	
		3	0.050		0.044	
	3	1	0.044	0.0450	0.044	0.0427
		2	0.047		0.043	
		3	0.044		0.041	
3	1	1	0.047	0.0477	0.045	0.0453
		2	0.048		0.045	
		3	0.048		0.046	
	2	1	0.048	0.0483	0.047	0.0463
		2	0.048		0.047	
		3	0.049		0.045	

Table D-1 (continued)

Run no. i	Sample no. j	Trial no. k	Light Water Solution: Absorbance readings A_{ijk}	Light Water Solution: Mean of absorbance readings A_{ij}	Heavy Water Solution: Absorbance readings A_{ijk}	Heavy Water Solution: Mean of absorbance readings A_{ij}
		1	0.049		0.048	
	3	2	0.050	0.0493	0.049	0.0483
		3	0.049		0.048	
		1	0.055		0.057	
	1	2	0.055	0.0553	0.057	0.0573
		3	0.056		0.058	
		1	0.056		0.055	
4	2	2	0.056	0.0567	0.054	0.0547
		3	0.058		0.055	
		1	0.058		0.058	
	3	2	0.057	0.0573	0.058	0.0583
		3	0.057		0.059	
		1	0.071		0.068	
	1	2	0.071	0.0713	0.068	0.0683
		3	0.072		0.069	
		1	0.073		0.069	
5	2	2	0.073	0.0733	0.069	0.0687
		3	0.074		0.068	

Table D-1 (continued)

Run no. i	Sample no. j	Trial no. k	Light Water Solution: Absorbance readings A_{ijk}	Light Water Solution: Mean of absorbance readings A_{ij}	Heavy Water Solution: Absorbance readings A_{ijk}	Heavy Water Solution: Mean of absorbance readings A_{ij}
		1	0.098		0.068	
	3	2	0.098	0.0977	0.069	0.0683
		3	0.097		0.068	
		1	0.059		0.057	
	1	2	0.059	0.0593	0.057	0.0573
		3	0.060		0.058	
		1	0.059		0.057	
6	2	2	0.059	0.0587	0.058	0.0573
		3	0.058		0.057	
		1	0.060		0.058	
	3	2	0.059	0.0593	0.057	0.0570
		3	0.059		0.056	

APPENDIX E

Statistical Analysis of the Raw Data of the Fast-Neutron Radiolysis Experiment

The analysis employed is that given in Chapter 2 of reference (2). The nomenclature of the symbols used appears at the end of this Appendix. The sample calculation given here is for the absorbance readings of the three light water samples in Run 1. Table E-1 shows the method by which the 95% confidence limits of the population means of absorbances of each sample were calculated.

The 95% confidence limit of the population mean was calculated from the equation:

$$"t" = \frac{\bar{A}_i - \bar{\bar{A}}_i}{s_{i,m}} \qquad \text{(E-1)}$$

The three values $\bar{A}_i$ shown in Table E-1 do not fall within the limits of each other. In order to elicit more information, the "L_1" test and the "F" test were carried out.

"L_1" Test. "L_1" for a set of data is given by the equation:

$$"L_1" = \frac{n_i [\Pi(s_i^2)]^{1/n_i}}{\sum(s_i^2)} \qquad \text{(E-2)}$$

The calculated value of "L_1" equals 0.719. From "L_1" tables, "L_1" = 0.3040 at 5% level and "L_1" = 0.1615 at 1% level. This means that the probability for the population variances to be the same is greater than 5%.

"F" Test. "F" is calculated from the following equation:

$$s_e^2 = \frac{\sum_i^i \sum_j^j (A_{ij} - \bar{A}_i)^2}{\sum_i^i [(n_j)_i] n_i} \qquad \text{(E-3)}$$

$$\bar{A}_p = \frac{\sum_i^i (n_j)_i \bar{A}_i}{\sum_i^i (n_j)_i} \qquad \text{(E-4)}$$

$$s^2_{m,p} = \frac{\sum_i^i (\bar{A}_i - \bar{A}_p)^2}{(n_i - 1)} \qquad \text{(E-5)}$$

$$s^2_p = n_j s^2_{m,p} \qquad \text{(E-6)}$$

$$\text{"F" (calculated)} = \frac{s^2_p}{s^2_e} = 45.8 \qquad \text{(E-7)}$$

From tables "F" = 5.14 at 5% level and "F" = 10.92 at 1% level.

Since the calculated value of "F" is greater than 10.92, only in less than 1% of the cases could the observed differences in sample means be explained on the basis of the scatter of data. This means that one or more of the data sets have incurred a non-random error. Further analysis showed that the second set (i=2) should be rejected. Accepting sets 1 and 3, the mean absorbance was calculated by taking the average of $\bar{A}_1$ and $\bar{A}_3$. The deviation of the mean was taken as equal to half the square root of the

Table E-1. 95% Confidence Limits of the Population Mean $\bar{\bar{A}}_i$

1	2	3	4[a]	5[b]	6[c]	7[d]	8[e]
i	j	A_{ij}	$\bar{A}_i$	$10^8 \times (\bar{\sigma}_i^2)$	$10^8 \times s^2_i$	$10^8 \times s^2_{i,m}$	$\bar{\bar{A}}_i$
	1	.042					
1	2	.042	.0423	25.7	38.6	12.9	.0423 ± .0015
	3	.043					
	1	.052					
2	2	.052	.0513	89	134	44.5	.0513 ± .0029
	3	.050					
	1	.044					
3	2	.044	.0450	200	300	100	.0450 ± .0043
	3	.044					

a $\bar{A}_i = \frac{\sum A_{ij}}{3}$. b $\bar{\sigma}_i^2 = \frac{\sum (A_{ij} - \bar{A}_i)^2}{3}$. c $s^2_i = \frac{3}{2}(\bar{\sigma}_i^2)$. d $s^2_{i,m} = \frac{s^2_i}{3}$.

e This column gives the population means with the 95% confidence limits. The value of "t" is 4.303.

sum of the variances of $\bar{\bar{A}}_1$ and $\bar{\bar{A}}_3$. The calculated value of absorbance was found to be equal to 0.0435 $\pm$ 5.3 %.

This procedure was repeated for each run for both light water and heavy water samples. The results of the calculations are shown in Table E-2.

Nomenclature for Appendix E

A_{ij}	Absorbance of the i^{th} sample in j^{th} trial
$\bar{A}_i$	Sample mean of absorbances in the i^{th} sample
$\bar{\bar{A}}_i$	Population mean of absorbances of the i^{th} sample
$\bar{\bar{A}}_p$	A population mean defined by Eq. (E-4)
"F"	Defined by Eq. (E-7)
"L_1"	Defined by Eq. (E-2)
n_i	Number of samples in a run
n_j	Number of trials in a sample
$(n_j)_i$	Number of trials for the i^{th} sample
s^2_e	Estimate of error variance, defined by Eq. (E-3)
s^2_i	Sample estimate of the population variance of absorbances of the i^{th} sample
$s^2_{i,m}$	Sample estimate of the variance of a set of mean absorbances for the i^{th} sample
$s^2_{m,p}$	Variance of the population of means, defined by Eq. (E-5)
s^2_p	Defined by Eq. (E-6)
"t"	Student's "t", defined by Eq. (E-1)
$\bar{\sigma}_i^2$	Sample variance of absorbance of the i^{th} sample

Table E-2. Best Values of Absorbances in Runs

Run no.	Sample no.	Light Water: Absorbance of sample	Light Water: Absorbance in run	Heavy Water: Absorbance of sample	Heavy Water: Absorbance in run
	1	.0423 ± .0015			
1	2		.0435 ± .0023	.0457 ± .0052	.0437 ± .0020
	3	.0450 ± .0043		.0427 ± .0038	
	1	.0477 ± .0014		.0453 ± .0014	
3	2	.0483 ± .0014	.0484 ± .0008	.0463 ± .0029	.0466 ± .0011
	3	.0493 ± .0014		.0483 ± .0014	
	1	.0553 ± .0014		.0573 ± .0014	
4	2	.0567 ± .0029	.0564 ± .0011		.0578 ± .0010
	3	.0573 ± .0014		.0583 ± .0014	
	1	.0573 ± .0014		.0683 ± .0015	
5	2	.0733 ± .0015	.0723 ± .0010	.0687 ± .0015	.0684 ± .0009
	3			.0683 ± .0015	
	1	.0593 ± .0015		.0573 ± .0015	
6	2	.0587 ± .0015	.0591 ± .0009	.0573 ± .0015	.0572 ± .0015
	3	.0573 ± .0015		.0570 ± .0040	

APPENDIX F

Relative Nuclear Target Density for Scattering of Neutrons Created in the (n,2n) Reaction

The secondary neutron flux, created in the (n,2n) reaction, depends upon the volume and shape of the container. Since, in the final analysis, the amount of energy lost by these neutrons turns out to be small the relative target nuclear density is calculated in an approximate manner as follows.

The container is assumed to be a sphere whose volume is equal to that of the container actually used. A uniform spherical source of neutrons is assumed to be created by the (n,2n) reaction and is given by the equation:

$$S_v = 2N_d \sigma_{(n,2n)}, \qquad \text{(F-1)}$$

where S_v is the number of neutrons created per cm^3 per sec, per unit fast-neutron flux; N_d is the density of deuterium nuclei in heavy water, atoms per cm^3; and $\sigma_{(n,2n)}$ is the cross-section for the (n,2n) reaction, cm^2.

The flux of neutrons due to this source is a function of position in the sphere and is a maximum at the center. The maximum flux, $\phi_{max.}$, is given by the equation:

$$\phi_{max.} = S_v R_o, \qquad \text{(F-2)}$$

where R_o is the radius of the sphere. For the sake of simplicity, the maxi-

mum flux is used for calculations instead of the average flux.

The relative target nuclear density for scattering of the secondary neutrons is then equal to $\phi_{max.} \times \frac{2}{3}$ or $2N_d\ \sigma_{(n,2n)}\ R_o \times \frac{2}{3}$. Substituting the numerical values:

$$2N_d\ \sigma_{(n,2n)}\ R_o \times \frac{2}{3} = 2 \times (6.02 \times 10^{23} \times \frac{1}{20} \times 1.1 \times 2)$$

$$\times\ (0.2 \times 10^{-24}) \times 2.2 \times \frac{2}{3} = 38.7 \times 10^{-3}.$$

FAST-NEUTRON RADIOLYSIS OF HEAVY WATER

by

SAMPATH SADHU KUMAR

B. Sc. (Tech.), MADRAS UNIVERSITY, INDIA, 1956.

AN ABSTRACT OF
A MASTER'S THESIS

submitted in partial fulfillment of the

requirements for the degree

MASTER OF SCIENCE

Department of Nuclear Engineering

KANSAS STATE UNIVERSITY

Manhattan, Kansas

1967

ABSTRACT

The G-value for the oxidation of Fe^{2+} ions to Fe^{3+} ions induced in the heavy water Fricke dosimeter by 14.6 Mev. neutrons was experimentally determined. The $G(Fe^{3+})$-value was found to be equal to 11.1 ± 1.0 ions per 100 ev. This was based on a published result of $G(Fe^{3+})$-value of 10.5 for the fast-neutron induced oxidation in light water. The G-value was computed from the measured ratio of absorbances, at a wavelength of 305 mμ, of heavy water and light water solutions exposed to the same time-integrated neutron flux.

The G-value for heavy water is based on a calculated value of the ratio of the first collision dose rates in light water and heavy water, and also on the published value of the ratio of the extinction coefficients of Fe^{3+} ions in heavy water and light water solutions.

The n-d elastic scattering was analyzed from the published data of differential cross-sections. The insufficient data on the differential cross-sections for the (n,2n) reaction necessitated certain approximations in its analysis. The calculated ratio of first collision dose rates in light water and heavy water was 1.165. The ratio of the extinction coefficients of Fe^{3+} ions in heavy water and light water was taken to be 1.068.

The fast-neutron radiolysis experiment was preceded by the two experiments: a) determination of the extinction coefficients for Fe^{3+} ions in water (containing 0.8N H_2SO_4) and b) determination of the $G(Fe^{3+})$-value of heavy water (containing 0.8N H_2SO_4) for Co-60 gamma radiolysis. The value of the extinction coefficient for ferric ions was found to be equal to 2118 liters per mole-cm. at 25°C. The $G(Fe^{3+})$-value was found to be equal to 16.8 for Co-60 gamma radiolysis of heavy water.